Neuron

Article

Top-down control of the descending pain modulatory system drives multimodal placebo analgesia

Graphical abstract

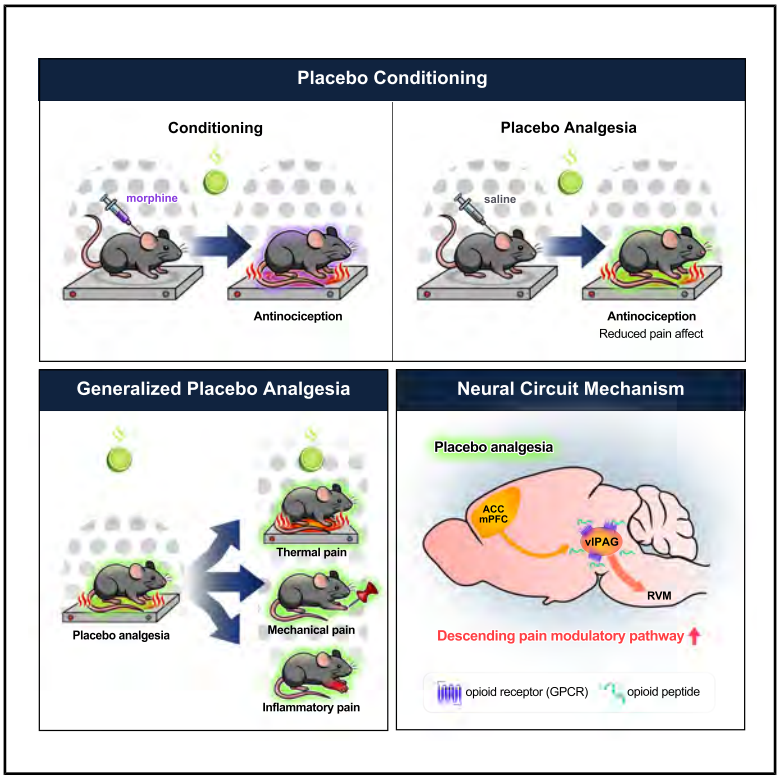

Highlights

- Descending vlPAG neurons control both morphine and placebo analgesia
- Cortical input to PAG is required for placebo but not morphine analgesia
- Endogenous opioids in the vlPAG gate placebo analgesia
- Placebo generalizes across pain types and builds resilience to injury-induced pain

Authors

Giulia Livrizzi, Janie Chang-Weinberg, Desiree A. Johnson, ..., Gregory Corder, Lin Tian, Matthew R. Banghart

Correspondence

mbanghart@ucsd.edu

In brief

Livrizzi, Chang-Weinberg, et al. identify a cortical-brainstem circuit that mediates top-down control of pain during placebo analgesia and fin that pain relief is gated by endogenous opioids in the vlPAG. They fin that the placebo effect extends to multiple forms of pain and that pre-conditioning promotes pain resilience after injury.

Livrizzi et al., 2026, Neuron *114*, 1–17
August 19, 2026 © 2026 The Author(s). Published by Elsevier Inc.
https://doi.org/10.1016/j.neuron.2026.03.025

CellPress

Please cite this article in press as: Livrizzi et al., Top-down control of the descending pain modulatory system drives multimodal placebo analgesia, Neuron (2026), https://doi.org/10.1016/j.neuron.2026.03.025

Neuron

CellPress
OPEN ACCESS

Article

Top-down control of the descending pain modulatory system drives multimodal placebo analgesia

Giulia Livrizzi,[1,2,13] Janie Chang-Weinberg,[1,2,13] Desiree A. Johnson,[1] Susan T. Lubejko,[1,3] Jingzhu Liao,[1] Blake A. Kimmey,[4,5,6] Chunyang Dong,[7] Yuan Li,[8] Kevin T. Beier,[8,9,10,11] Gregory Corder,[4,5,6] Lin Tian,[7,12] and Matthew R. Banghart[1,14,*]

[1]Department of Neurobiology, School of Biological Sciences, University of California San Diego, La Jolla, CA 92093, USA
[2]Biological Sciences Graduate Program, University of California San Diego, La Jolla, CA, USA
[3]Neurosciences Graduate Program, University of California San Diego, La Jolla, CA, USA
[4]Department of Psychiatry, Perelman School of Medicine, University of Pennsylvania, Philadelphia, PA 19104, USA
[5]Department of Neuroscience, Mahoney Institute for Neurosciences, Perelman School of Medicine, University of Pennsylvania, Philadelphia, PA 19104, USA
[6]Department of Anesthesiology and Critical Care, Perelman School of Medicine, University of Pennsylvania, Philadelphia, PA 19104, USA
[7]Department of Biochemistry and Molecular Medicine, School of Medicine, University of California, Davis, Davis, CA 95817, USA
[8]Department of Physiology and Biophysics, University of California, Irvine, Irvine, CA 92617, USA
[9]Department of Biomedical Engineering, University of California, Irvine, Irvine, CA 92617, USA
[10]Department of Neurobiology and Behavior, University of California, Irvine, Irvine, CA 92617, USA
[11]Department of Pharmaceutical Sciences, University of California, Irvine, Irvine, CA 92617, USA
[12]Max Planck Florida Institute for Neuroscience, Jupiter, FL 33458, USA
[13]These authors contributed equally
[14]Lead contact
*Correspondence: mbanghart@ucsd.edu
https://doi.org/10.1016/j.neuron.2026.03.025

SUMMARY

Placebo analgesia, in which expectation and prior experience suppress pain in response to an inert treatment, is a powerful clinical phenomenon whose causal neural basis remains unclear. By reverse-translating a human placebo paradigm to mice, we identify neural circuits linking the cortex to the brainstem that causally mediate placebo pain relief. Placebo conditioning suppresses both nociceptive and affective-motivational pain behaviors and generalizes to unconditioned forms of pain. Descending neurons in the ventrolateral periaqueductal gray (vlPAG) are indispensable for both morphine and placebo analgesia, but the placebo effect additionally requires medial prefrontal and anterior cingulate cortical inputs to the vlPAG. Conditioning potentiates noxious stimulus-evoked endogenous opioid release in the vlPAG, which causally gates descending pain modulation. Remarkably, conditioning in pain-naive animals produces lasting placebo analgesia after injury. These findings identify a central circuit mechanism of placebo analgesia and suggest a translational strategy in which preventive placebo conditioning can build resilience to pain.

INTRODUCTION

Placebo analgesia is a form of cognitive pain modulation in which expectations and prior experience suppress pain in response to an inert treatment.[1–5] In humans, placebo effects can be induced through conditioning, verbal suggestion, or contextual cues, and they contribute substantially to analgesic efficacy in both experimental and clinical settings. At the same time, placebo responses complicate the interpretation of clinical trials and obscure drug effects, underscoring the need to understand their underlying neurobiology.[5,6] A neural mechanistic understanding of placebo analgesia could enable these endogenous pain-suppressing processes to be deliberately engaged for therapeutic benefit, potentially reducing reliance on opioid drugs for pain.[7,8]

Human neuroimaging studies have implicated a distributed network of cortical and subcortical regions in placebo analgesia, including the medial prefrontal cortex (mPFC), anterior cingulate cortex (ACC), anterior insular cortex (AI), and the periaqueductal gray (PAG).[9–12] Endogenous opioid signaling appears to play a central role, as placebo analgesia is commonly blocked by opioid receptor antagonists[4,13,14] and is associated with opioid peptide release detected by positron emission tomography.[15,16] Notably, many of these same regions are engaged by exogenous opioid analgesics such as morphine, suggesting that placebo and drug-induced analgesia may converge on a shared pain modulatory system.[17] However, because these conclusions are drawn largely from correlative measurements in humans, the causal roles of specific neural

This is an open access article under the CC BY-NC license (http://creativecommons.org/licenses/by-nc/4.0/).

Please cite this article in press as: Livrizzi et al., Top-down control of the descending pain modulatory system drives multimodal placebo analgesia, Neuron (2026), https://doi.org/10.1016/j.neuron.2026.03.025

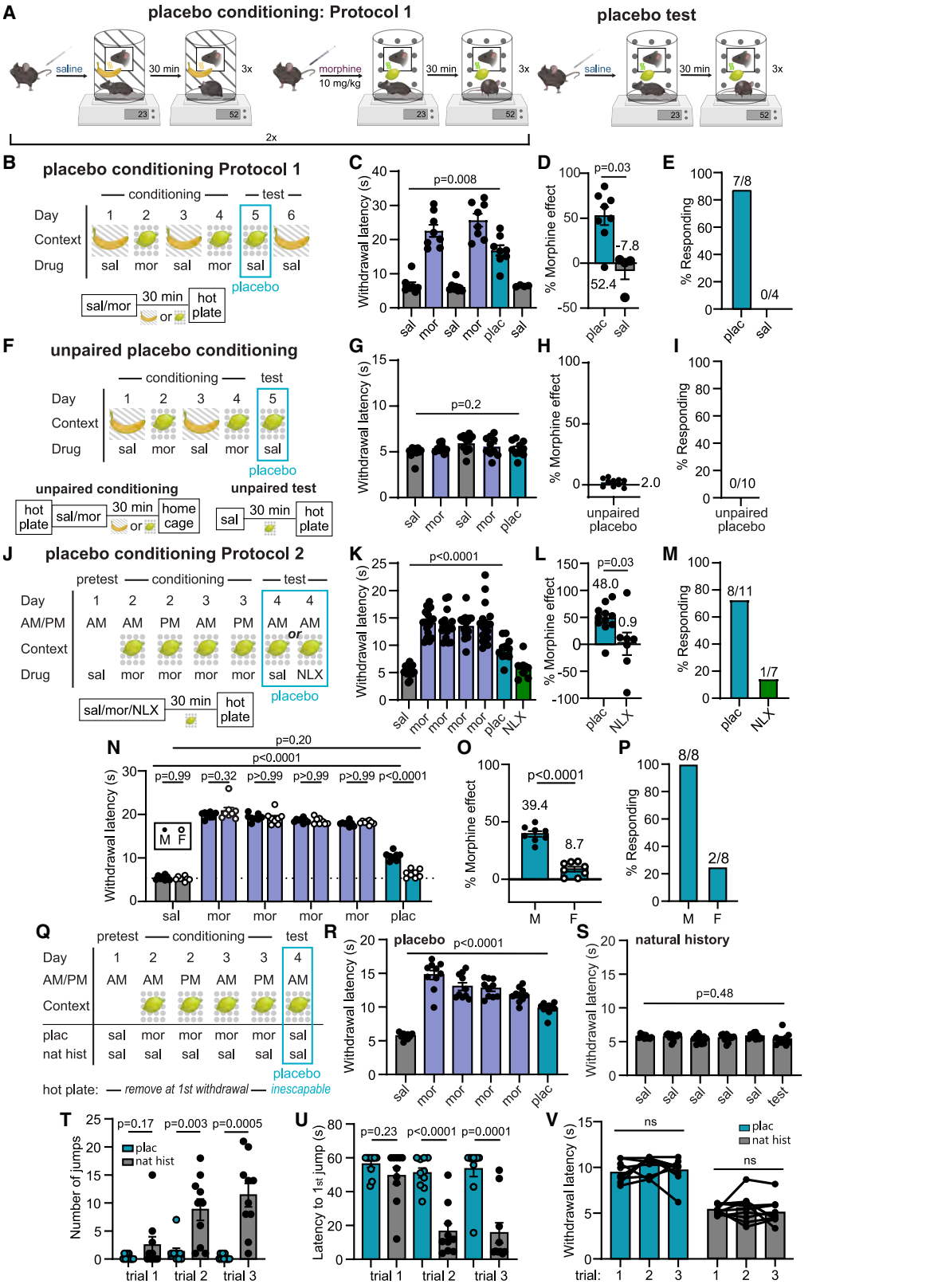

(legend on next page)

Please cite this article in press as: Livrizzi et al., Top-down control of the descending pain modulatory system drives multimodal placebo analgesia, Neuron (2026), https://doi.org/10.1016/j.neuron.2026.03.025

CellPress
OPEN ACCESS

circuits—and their necessity for placebo analgesia—remain unresolved.[9,10,18,19]

Whether placebo analgesia suppresses pain by engaging the descending pain modulatory system is an important open question. Human imaging and pharmacology studies implicate endogenous opioids in placebo responses, yet it is still debated whether placebo analgesia is implemented through brainstem-mediated modulation of nociception or instead arises primarily from changes in pain appraisal without direct engagement of canonical descending control circuits.[20–25] A central hub in the descending pathway is the ventrolateral PAG (vlPAG), which inhibits spinal nociceptive processing via projections to the rostroventromedial medulla (RVM) and the locus coeruleus.[26–30] Although direct evidence is limited, vlPAG→RVM neurons are thought to be recruited by opioids through disinhibition.[31,32] Consistent with this model, activation of glutamatergic vlPAG neurons is analgesic.[33,34] Furthermore, we recently showed that ~85% of vlPAG→RVM neurons are glutamatergic and that activity in vlPAG$^{vGlut2\text{-}Cre}$ neurons is required for systemic morphine antinociception on the hot plate via spinal opioidergic and noradrenergic signaling.[30] These observations raise a key knowledge gap: whether placebo analgesia similarly depends on the vlPAG-centered descending circuitry and, if so, which upstream pathways and neuromodulatory signals recruit it.

An additional unresolved issue concerns the generalization of placebo effects, which is a hallmark of placebo in humans. In clinical trials, patients typically experience placebo analgesia despite not having been explicitly conditioned with the experimental drug within the same clinical context. This implies that expectancy-driven placebo effects generalize beyond the original learning conditions.[35,36] Recently, evidence for the generalization of placebo analgesia across pain modalities has emerged as well.[37,38] Whether rodent models capture the propensity of placebo analgesia to generalize is unknown.

Here, by reverse-translating a morphine-conditioned placebo paradigm from humans to mice, we identified cortico-brainstem pathways and endogenous opioid neuromodulatory signals that drive placebo analgesia.

RESULTS

Morphine-conditioned placebo analgesia in mice

To study the circuit mechanisms of placebo analgesia in mice, we established reliable placebo conditioning protocols based on contextual conditioning with morphine, under the premise that contextual cues associated with morphine-induced pain relief might promote pain suppression in the absence of drug treatment. Morphine conditioning has proven highly effective at producing placebo analgesia in human subjects.[4,39] Notably, placebo analgesia can involve reductions in the subjective experience of pain in addition to reductions in the neural or behavioral responses to noxious stimuli (antinociception). Although not studied intensively, contextual conditioning with morphine also produces context-evoked placebo antinociception in rodents.[14,40–42] In our conditioning protocols, mice were injected either with morphine or inert saline and then placed into multisensory contexts distinguished by both visual and olfactory cues (Figure 1A). After a 30 min wait period to achieve maximal

Figure 1. Contextual conditioning with morphine and pain produces endogenous opioid-dependent placebo analgesia in male mice

(A) Illustration of placebo conditioning protocols based on contextual conditioning with morphine on the hot plate. Chambers are distinguished by both visual (stripes or dots) and olfactory (banana or lemon) cues.
(B) Schematic describing protocol 1. The lower panel indicates the sequence of events on each day.
(C) Hot plate paw withdrawal latencies before, during, and after conditioning (n = 8 mice, only 4 of which were tested on day 6, Repeated Measures (RM) mixed effects model with Dunnett's post hoc, $F(2.39,14.82) = 40.58$, $p < 0.0001$).
(D) Placebo effect quantified as % of the response to the previous dose of morphine (Mann-Whitney test, see STAR Methods). The average % morphine effect is indicated above or below each bar.
(E) Placebo response quantified as the % of subjects exhibiting antinociception.
(F) Schematic describing the unpaired conditioning protocol that separates the hot plate test from the morphine context.
(G) Paw withdrawal latencies on the hot plate across unpaired conditioning and placebo test days (n = 10, RM one-way ANOVA with Dunnett's post hoc, $F(3.25,29.26) = 4.33$, $p = 0.011$).
(H) Same as in (D), but for the data shown in (G).
(I) Same as in (E), but for the data shown in (G).
(J) Schematic of protocol 2, including naloxone (NLX) administration on test day.
(K) Same as (C), but for protocol 2 (n = 18 mice total, placebo: n = 11, naloxone: n = 7, RM mixed-effects model with Dunnett's post hoc, $F(6,84) = 50.85$, $p < 0.0001$).
(L) Same as (D), but for the data shown in (K) (saline n = 11, naloxone n = 7, unpaired t test).
(M) Same as (E), but for the data shown in (K).
(N) Same as (K), but comparing male and female mice (male: n = 8, female: n = 8, one-way ANOVA with Sidak's post hoc, $F(11,84) = 309.1$, $p < 0.0001$). The dotted line indicates average baseline withdrawal latency (5.36 s).
(O) Same as (L), but comparing male and female responses (male: n = 8, female: n = 8, unpaired t test).
(P) Same as (M), but comparing male and female responses.
(Q) Schematic of protocol 2 adapted to measure escape behaviors by transitioning to the inescapable hot plate test on placebo test day.
(R) Hot plate paw withdrawal latencies before, during, and after conditioning for the placebo group (n = 10 per group, RM one-way ANOVA with Dunnett's post hoc, $F(2.41,21.64) = 71.40$, $p < 0.0001$).
(S) Same as (R), but for the natural history group (n = 10 per group, RM one-way ANOVA with Dunnett's post hoc, $F(2.56,23.0) = 1.17$, $p = 0.34$).
(T) The number of jumps across trials (n = 10 per group, RM two-way ANOVA with Tukey's post hoc, group × trial interaction $F(1.73,31.2) = 6.83$, $p = 0.005$).
(U) Latency to first jump across trials (n = 10 per group, RM two-way ANOVA with Tukey's post hoc, group × trial interaction $F(1.54,27.7) = 13.8$, $p = 0.0002$).
(V) Paw withdrawal latencies compared across trials for the morphine and natural history groups on placebo/test day (n = 10 per group, RM two-way ANOVA with Tukey's post hoc, group × trial interaction $F(1.98,35.7) = 0.61$, $p = 0.55$, group $F(1,18) = 128.3$, $p < 0.0001$).

Please cite this article in press as: Livrizzi et al., Top-down control of the descending pain modulatory system drives multimodal placebo analgesia, Neuron (2026), https://doi.org/10.1016/j.neuron.2026.03.025

morphine antinociception, three hindpaw withdrawal latencies were measured on a noxious temperature-controlled plate as a metric of thermal pain sensitivity (hot plate test). Importantly, on each trial, mice were removed promptly after exhibiting the first paw withdrawal to prevent sensitization to the assay. After conditioning, the placebo test consisted of inert saline administration and placement in the previously morphine-paired context prior to the hot plate test.

In placebo conditioning protocol 1, male mice were conditioned over 4 days with two exposures each to either morphine (10 mg/kg intraperitoneal [i.p.]) or saline (Figure 1B). This conditioning protocol produced strong placebo antinociception (52.4% ± 10.0%), quantified as the percent of the paw withdrawal latency increase produced by the prior dose of morphine (Figures 1C and 1D; the average of three consecutive trials is shown for each subject). In a subset of mice, subsequent saline administration in the saline context demonstrated that the placebo effect is context-specific. We also categorized subjects as either responders or non-responders (see STAR Methods) (Figure 1E). Considering responders only, this conditioning protocol produced 60.5% ± 6.8% of the morphine-induced antinociception.

To ask if the observed placebo effect is simply a consequence of context-evoked, non-pain-specific endogenous opioid release,[40,43,44] we employed an unpaired conditioning protocol that decoupled the association between morphine context and pain suppression (Figures 1F–1I). Mice were tested on the hot plate prior to morphine administration and subsequent contextual conditioning so that they learned to associate the context with morphine but never experienced analgesia on the hot plate. On test day, saline administration in the morphine context before the hot plate test failed to evoke placebo antinociception. These results demonstrate that contextual conditioning with morphine in the absence of a noxious stimulus is insufficient to produce placebo antinociception but instead requires [morphine + noxious stimulus]-conditioning and further suggest that the placebo effect is driven by a pain-predictive process.

In placebo conditioning protocol 2, we omitted the intermittent saline injections and increased the number of [morphine + noxious stimulus] exposures by administering morphine in both the morning and afternoon (Figure 1J). This protocol produced a placebo effect similar to protocol 1 (Figures 1K–1M). Consistent with a critical role for endogenous opioids,[4,13,14] treatment with naloxone (3 mg/kg i.p.) on test day completely abolished the placebo effect. Consistent with findings in healthy human subjects,[45] placebo antinociception efficacy was lower in female mice compared with male mice, despite morphine producing similar antinociception during conditioning (Figures 1N–1P). A sex difference in opioid-induced hyperalgesia (OIH) in response to the conditioning protocol is unlikely to account for the sex difference in placebo antinociception, as no OIH was observed in either sex (Figure S1A). As a result, subsequent mechanistic studies were performed exclusively in male mice.

Placebo antinociception was not accompanied by morphine-associated behaviors such as locomotor activation or Straub tail (Figure S1B), confirming that this placebo effect is unlikely to result from a context-evoked global opioid state.[40] We also found that decreasing the wait time between the saline injection and the hot plate test from 30 to 10 min on the placebo test day abolished the placebo effect (Figures S1C–S1F). Repeated testing once per day for several days caused the placebo response to extinguish with a time constant of 0.8 sessions (three trials per session), and reconditioning with two [morphine + noxious stimulus] exposures reinstated it to its initial magnitude (Figures S1G–S1J). Notably, the placebo effect size for individual mice and their rank order within the cohort changed after reconditioning, suggesting that individual mice may not be intrinsically more or less sensitive to placebo effects. Together, these findings indicate that the placebo antinociception induced by [morphine + noxious stimulus] conditioning depends on contextual and temporal discrimination.

To determine if the placebo effect also involves reductions in affective and/or emotional-motivational components of pain, we measured escape-related behaviors using the inescapable hot plate assay. After conditioning for the suppression of paw withdrawals, which assesses the sensory-discriminative component of pain (nociception), the inescapable hot plate assay was evaluated on the placebo test day only. A natural history group was contextually conditioned with saline instead of morphine as a control (Figure 1Q). Strikingly, in addition to the increased paw withdrawal latency (Figures 1R and 1S), mice in the placebo group exhibited reduced jumping behavior (Figure 1T) and an increased latency to the first jump (Figure 1U) in comparison to the natural history control mice. This was particularly apparent on trials 2 and 3, wherein control mice sensitized to the assay, increasing their jumping behavior over subsequent trials, whereas the morphine-conditioned placebo group did not. Notably, the initial paw withdrawal latency was stable across trials in both groups (Figure 1V), despite the apparent increase in motivation to escape in the natural history control group. These results suggest that conditioning for the suppression of nociception-driven paw withdrawals also suppresses affective-motivational components of pain and therefore produces analgesia, in addition to antinociception. By suppressing the aversive qualities of the noxious stimulus, the placebo effect may also suppress the aversive learning that occurs across individual trials to expedite escape behaviors. Furthermore, because the suppression of escape-like jumping behavior was not included in the conditioning protocol, wherein mice were removed from the hot plate immediately after the first paw withdrawal, this form of [morphine + noxious stimulus]-conditioned placebo analgesia does not simply reflect a conditioned motor response.

Placebo analgesia relies on the descending pain modulatory system

To determine if descending pain modulatory circuits are engaged during [morphine + noxious stimulus]-conditioned placebo analgesia, we implemented an activity-dependent genetic trapping approach.[46] Our primary goal was to ask if activity in vlPAG neurons that are activated by the [morphine + noxious stimulus]-conditioned context on placebo day is sufficient to produce antinociception. Several weeks prior to conditioning, TRAP2 (Fos2A-iCreER) mice were bilaterally transduced in the vlPAG with a Cre-dependent adenoassociated virus (AAV) encoding the excitatory designer receptor exclusively activated by designer drugs (DREADD) hM3Dq-mCherry[47] (Figure 2A). Mice

Please cite this article in press as: Livrizzi et al., Top-down control of the descending pain modulatory system drives multimodal placebo analgesia, Neuron (2026), https://doi.org/10.1016/j.neuron.2026.03.025

CellPress
OPEN ACCESS

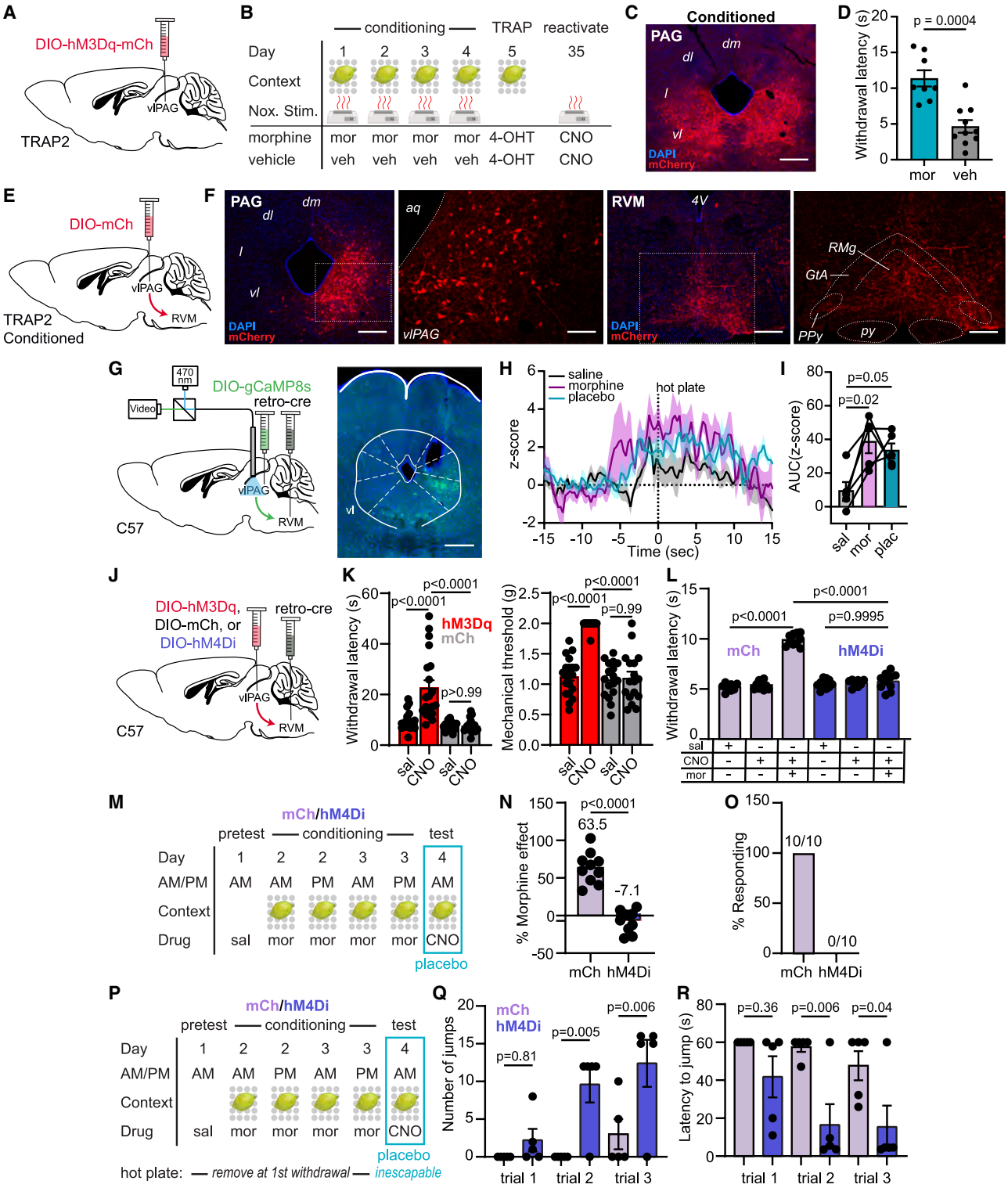

Figure 2. Pain modulatory vlPAG → RVM neurons support morphine antinociception and morphine-conditioned placebo analgesia

(A) Illustration of viral labeling of vlPAG neurons with hM3Dq-mCherry in TRAP2 mice.

(B) Schematic of the placebo protocol used for chemogenetic reactivation of neurons active in the [morphine + noxious stimulus]-conditioned context.

(C) Representative image of viral expression post injection. Scale bar, 400 μm.

(legend continued on next page)

Please cite this article in press as: Livrizzi et al., Top-down control of the descending pain modulatory system drives multimodal placebo analgesia, Neuron (2026), https://doi.org/10.1016/j.neuron.2026.03.025

were again conditioned by administering morphine (10 mg/kg i.p.) 30 min prior to placement on the hot plate. The negative control group received vehicle during conditioning (see Figures S2A and S2B for hot plate data obtained from a separate cohort of mice). To allow for the expression of Cre-recombinase in neurons that are highly active in the conditioned context, mice were administered 4-hydroxytamoxifen (4-OHT; 20–40 mg/kg, subcutaneous [s.c.]) prior to placement in the [morphine + noxious stimulus]-conditioned or [saline + noxious stimulus]-conditioned contexts (Figure 2B). After several weeks of expression, this led to strong hM3Dq-mCherry expression in the vlPAG (Figure 2C). Activation of hM3Dq-expressing neurons with clozapine N-oxide (CNO) (3 mg/kg i.p.) 30 days later produced greater antinociception on the hot plate in the [morphine + noxious stimulus]-conditioned mice than [saline + noxious stimulus]-conditioned mice (Figure 2D). Unilateral labeling of [morphine + noxious stimulus]-trapped neurons with mCherry revealed bilateral projections to the RVM (Figures 2E and 2F). Together, these results indicate that [morphine + noxious stimulus]-contextual conditioning leads to context-driven reactivation of a stable, functionally defined population of vlPAG neurons that can be re-engaged to elicit antinociception, even weeks after conditioning.

To understand how pain-related neural activity in the vlPAG is altered by placebo conditioning, we recorded hot plate-evoked Ca^{2+} activity from anatomically defined vlPAG→RVM projection neurons using fiber photometry before, during, and after [morphine + noxious stimulus] conditioning. Bilateral injection of AAVretro-Cre[48] in the RVM and unilateral Cre-dependent jGCaMP8s[49] in the vlPAG provided access to vlPAG→RVM projection neurons (Figure 2G). Notably, we observed the initiation of Ca^{2+} activity in vlPAG→RVM neurons during the process of transferring the mouse to the hot plate (Figure 2H), which may reflect the vlPAG's role in threat processing.[50] It subsequently remained elevated during exposure to the noxious stimulus. This hot plate-evoked Ca^{2+} activity was enhanced after morphine treatment (10 mg/kg i.p.) as well as during the placebo test (Figure 2I). These data reveal facile activation of vlPAG→RVM neurons in states of opioid-dependent analgesia and are consistent with opioid-mediated disinhibition of vlPAG→RVM neurons.

We next sought to determine whether activity in vlPAG→RVM neurons plays a causal role in placebo analgesia using chemogenetics. We first established that chemogenetic activation of anatomically defined vlPAG→RVM neurons with hM3Dq produces strong antinociception on the hot plate as well as in the von Frey assay of mechanical nociception (Figures 2J, 2K, and S2C). Chemogenetic silencing of vlPAG→RVM neurons with hM4Di prevented morphine antinociception at a dose of 5 mg/kg i.p. (Figures 2L, S2D, and S2E), consistent with prior findings inhibiting a broader population of $vlPAG^{vGlut2\text{-}Cre}$ neurons.[30] At higher doses of morphine (10 and 20 mg/kg i.p.), silencing vlPAG→RVM neurons did not attenuate antinociception, presumably due to direct activation of spinal opioid receptors (Figure S2F). Strikingly, chemogenetic silencing of either vlPAG→RVM neurons (Figures 2M–2O and S2G) or $vlPAG^{vGlut2\text{-}Cre}$ neurons (Figures S2H–S2M) on placebo test day completely blocked placebo antinociception. Chemogenetic silencing of vlPAG→RVM neurons also reversed the placebo-driven suppression of unconditioned escape-like jumping behavior (Figures 2P–2R). These results establish that [morphine + noxious stimulus]-conditioned placebo analgesia, similar to morphine antinociception, requires engagement of the descending pain modulatory system through the vlPAG.

Neural pathways for top-down pain modulation

Although multiple cortical structures are implicated in placebo pain relief, it is not clear how the PAG receives top-down information that drives descending pain modulation. To identify candidate input structures, we first mapped the synaptic inputs

(D) Hot plate paw withdrawal latency following chemogenetic reactivation of TRAPed neurons on day 35 (morphine-conditioned: $n = 8$, vehicle-conditioned: $n = 10$, unpaired t test).
(E) Illustration of viral labeling of vlPAG neurons with mCherry in TRAP2 mice for anatomical mapping of neurons activated by the [morphine + noxious stimulus]-conditioned context.
(F) Representative images of TRAPed neurons from (E) demonstrating labeling of neurons in the vlPAG with projections to the RVM. Scale bar lengths: vlPAG (left) = 350 μm, vlPAG (right) = 170 μm, RVM (left) = 300 μm, RVM (right) = 250 μm.
(G) Illustration of the retrograde viral injection approach for fiber photometry recordings from vlPAG→RVM neurons (left) and an example of jGCaMP8s expression under the implanted optical fiber (right, scale bar, 500 μm).
(H) Average z-score of Ca^{2+} activity in vlPAG → RVM neurons upon exposure to the hot plate over the course of conditioning (protocol 2, $n = 5$).
(I) Quantification of the Ca^{2+} activity shown in (H) (integration window: −5 to 15 s, RM one-way ANOVA with Holm-Sidak's post hoc, $F(1.69,6.75) = 7.37$, $p = 0.022$).
(J) Illustration of the retrograde viral approach for DREADD expression in vlPAG → RVM neurons.
(K) Paw withdrawal latencies on the hot plate (left) and mechanical thresholds to stimulation with von Frey fibers (right) upon chemogenetic activation of vlPAG → RVM neurons with hM3Dq vs. mCherry control (male and female mice combined, hM3Dq: $n = 20$, mCh: $n = 17$, HP: One-way ANOVA with Sidak's post hoc, $F(3,70) = 19.64$, $p < 0.0001$; VF: One-way ANOVA with Sidak's post hoc, $F(3,70) = 43.36$, $p < 0.0001$), $^{****}p < 0.0001$.
(L) Hot plate paw withdrawal latencies in response to saline, CNO (3 mg/kg i.p.), and morphine (5 mg/kg i.p.) administration upon chemogenetic inactivation of vlPAG → RVM neurons with hM4Di vs. mCherry control (mCh: $n = 10$, hM4Di: $n = 10$, two-way ANOVA with Tukey's post hoc, drug × virus interaction $F(5,108) = 5.49$, $p = 0.0002$).
(M) Schematic of placebo protocol 2 indicating chemogenetic silencing with CNO administration on placebo test day.
(N) Placebo effect quantified as % of the response to the previous dose of morphine upon chemogenetic silencing of vlPAG → RVM neurons (mCh: $n = 10$, hM4Di: $n = 10$, unpaired t test).
(O) Placebo response in (N) quantified as the % of subjects exhibiting antinociception.
(P) As in (M), but to measure escape behavior on the placebo test day.
(Q) The number of jumps across trials upon chemogenetic silencing of vlPAG → RVM neurons (mCh: $n = 5$, hM4Di: $n = 5$, one-way ANOVA with Sidak's post hoc, $F(5,24) = 7.56$, $p = 0.0002$).
(R) Latency to first jump across trials (one-way ANOVA with Sidak's post hoc, $F(5,24) = 5.42$, $p = 0.002$).

Please cite this article in press as: Livrizzi et al., Top-down control of the descending pain modulatory system drives multimodal placebo analgesia, Neuron (2026), https://doi.org/10.1016/j.neuron.2026.03.025

CellPress
OPEN ACCESS

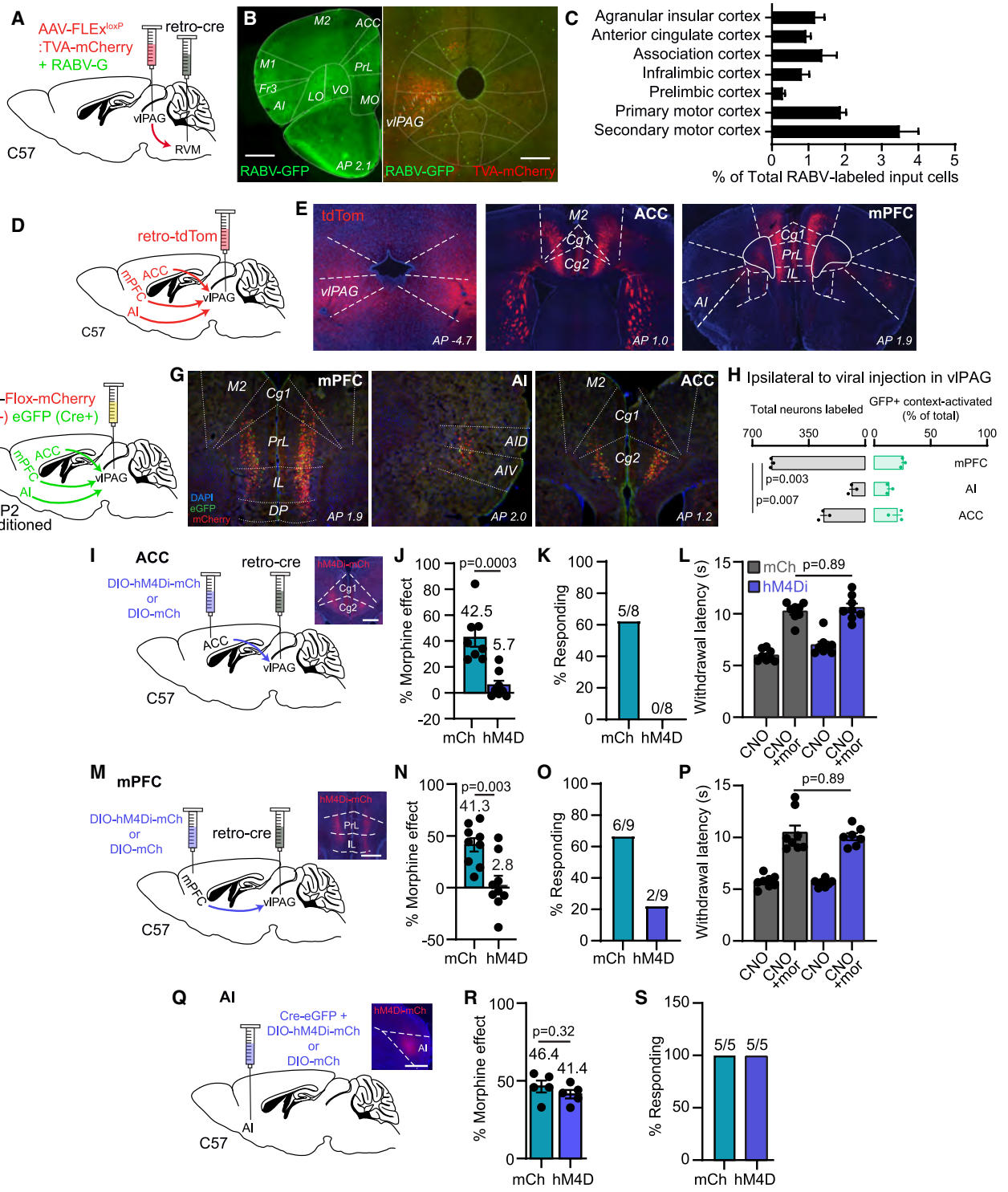

Figure 3. Cortical input to the PAG is critical for placebo antinociception

(A) Illustration of the RABV-mediated trans-synaptic tracing approach for identifying brain regions that synapse onto vlPAG → RVM neurons.

(B) Representative image of an anterior cortical section containing many labeled cells (left, scale bar, 500 μm) and the injection site within the vlPAG (right, scale bar, 350 μm).

(C) Plot summarizing the cortical regions identified as providing synaptic input to vlPAG → RVM neurons (n = 6 mice).

(D) Illustration of retro-AAV tdTom injection into vlPAG for retrograde labeling of cortical inputs.

(legend continued on next page)

Please cite this article in press as: Livrizzi et al., Top-down control of the descending pain modulatory system drives multimodal placebo analgesia, Neuron (2026), https://doi.org/10.1016/j.neuron.2026.03.025

to vlPAG→RVM neurons using transsynaptic retrograde tracing with pseudotyped rabies virus (RABV) (Figure 3A). This experiment identified multiple cortical (Figures 3B and 3C) and subcortical (Figure S3A) structures that are poised to directly influence descending pain modulation. In the cortex, we observed labeling of neurons in the somatosensory areas, the primary and secondary motor nuclei, the agranular insula, the anterior cingulate, and the infralimbic (IL) region of the prefrontal cortex (PFC). Using AAVretro-tdTomato to access cortical inputs to the vlPAG, we observed dense labeling throughout the rostro-caudal axis of the ACC, the IL and prelimbic (PrL) cortices (collectively referred to here as the mPFC), the secondary motor cortex (M2), and the AI (Figures 3D and 3E).

To identify cortical inputs to the vlPAG that are active during placebo analgesia, we combined activity-dependent gene trapping with retrograde tracing using a Cre-dependent AAVretro reporter in TRAP2 mice (Figure 3F). We unilaterally injected the vlPAG with a dual-color reporter that labels Cre-expressing neurons with eGFP and Cre-negative neurons with mCherry[51] and trapped active neurons in the [morphine + noxious stimulus]-conditioned context as in Figure 2B. Histological analysis (Figure 3G) revealed eGFP and mCherry expression in the mPFC, ACC, and AI both ipsi- and contralateral to the vlPAG injection site, with the greatest eGFP expression in the ipsilateral hemisphere (quantified in Figure 3H). These results reveal that cortical input to the vlPAG from the mPFC, ACC, and AI is activated by the [morphine + noxious stimulus]-conditioned context. As each of these areas was also identified as providing direct input to antinociceptive vlPAG→RVM neurons using RABV, we hypothesized that they might causally contribute to placebo analgesia by driving descending pain modulation.

To determine the necessity of each projection pathway, we chemogenetically silenced vlPAG-projecting neurons located in the ACC, mPFC, and AI during the placebo test. vlPAG-projecting neurons in either the ACC or mPFC were labeled by bilaterally injecting AAVretro-Cre in the vlPAG, along with either Cre-dependent hM4Di or mCherry in the cortex, whereas the vlPAG-projecting region of AI was directly transduced with a mixture of Cre and either hM4Di or mCherry. Consistent with causal roles for the ACC and mPFC, placebo antinociception was blocked by inactivation of vlPAG-projecting neurons in the ACC and mPFC (Figures 3I–3K, S3B, 3M–3O, and S3C, respectively). However, silencing these pathways did not alter morphine antinociception (5 mg/kg i.p.; Figures 3L and 3P). In contrast to the ACC and mPFC inputs, inactivation of the vlPAG-projecting region of the AI had no effect on placebo antinociception (Figures 3Q–3S and S3D), consistent with the AI playing an evaluative rather than causal role in placebo analgesia.[9,15,52] To determine if these cortical inputs to the vlPAG are sufficient to drive antinociception, as has been observed for the mPFC→vlPAG pathway after injury,[53] we simultaneously activated both ACC→vlPAG and mPFC→vlPAG neurons bilaterally with hM3Dq. However, this failed to alter nociception using either the hot plate or von Frey assays (Figures S3E and S3F), despite triggering strong cFOS expression in the ACC and mPFC (Figures S3G–S3I).

Together, these results indicate that cortical inputs to the vlPAG from the ACC and the mPFC contribute causally to placebo antinociception. By contrast, cortical input to the vlPAG is not a key factor in the antinociception produced by opioid drugs. Yet, cortical input from the ACC and mPFC is unable to drive descending pain modulation through the vlPAG on its own, suggesting that an additional process is critical for triggering the circuit to produce placebo analgesia.

Endogenous opioid signaling in the vlPAG

Like most forms of placebo pain relief, [morphine + noxious stimulus]-conditioned placebo antinociception in mice relies on endogenous opioid signaling (Figures 1J–1M). We hypothesized that this signaling may occur in the vlPAG, as local administration of opioid agonists in the vlPAG activates descending pain modulatory circuitry to produce strong antinociception.[28,54] Although positron emission tomography (PET) imaging studies in humans suggest that endogenous opioid peptides are released in the

(E) Example images of the bilateral vlPAG injection sites (left, scale bar 400 μm) and labeled input neurons in the ACC (middle, scale bar 500 μm) and mPFC/AI (right, scale bar 750 μm).
(F) Illustration of the dual-color retro-AAV approach in TRAP2 mice for identifying cortical inputs to the vlPAG that are active in the [morphine + noxious stimulus]-conditioned context.
(G) Representative images of labeled neurons in mPFC (left, scale bar, 350 μm), AI (middle, scale bar, 400 μm), and ACC (right, scale bar, 500 μm).
(H) Graph summarizing the total number of mPFC, AI, and ACC neurons labeled with mCherry and the relative percentages of these cells labeled with GFP and thus identified as active in the [morphine + noxious stimulus]-conditioned context in each mouse (n = 3 mice, total neurons labeled: RM one-way ANOVA with Bonferroni's post hoc, F(1.04,2.07) = 261.7, p = 0.0032; GFP+ % of total: RM one-way ANOVA, F(1.05,2.1) = 11, p = 0.075).
(I) Illustration of the retrograde viral injection approach for chemogenetic silencing of ACC → PAG neurons. Inset: representative image of hM4Di-mCh expression in ACC (scale bar, 500 μm).
(J) Placebo effect quantified as % of the response to the previous dose of morphine upon chemogenetic silencing of ACC → PAG neurons (mCh: n = 8, hM4Di: n = 8, unpaired t test).
(K) Placebo response in (J) quantified as the % of subjects exhibiting antinociception.
(L) Hot plate paw withdrawal latencies upon chemogenetic inactivation of ACC → PAG neurons with hM4Di vs. mCherry control in response to CNO (3 mg/kg i.p.) or CNO + morphine (5 mg/kg) administration (mCh: n = 8, hM4Di: n = 8, RM one-way ANOVA with Sidak's post hoc, F(3,28) = 49.74, p < 0.0001).
(M) Same as (I), but for mPFC → PAG neurons (scale bar, 500 μm).
(N) Same as (J), but for mPFC → PAG neurons (mCh: n = 9, hM4Di: n = 9, unpaired t test).
(O) Same as (K), but for mPFC → PAG neurons.
(P) Same as (L), but for mPFC → PAG neurons (mCh: n = 8, hM4Di: n = 7, RM one-way ANOVA with Sidak's post hoc, F(3,26) = 39.90, p < 0.0001).
(Q) Same as in (I) for the PAG-projecting region of AI (scale bar 1 mm).
(R) Same as (J), but for the PAG-projecting region of AI (mCh: n = 5, hM4Di: n = 5, unpaired t test).
(S) Same as (K), but for the PAG-projecting region of AI.

Please cite this article in press as: Livrizzi et al., Top-down control of the descending pain modulatory system drives multimodal placebo analgesia, Neuron (2026), https://doi.org/10.1016/j.neuron.2026.03.025

CellPress
OPEN ACCESS

PAG along with many other brain regions during placebo analgesia,[15,16] a causal role for local opioid signaling has not been established. Furthermore, the temporal dynamics of opioid release during placebo trials remain undefined.

To determine if morphine-conditioned placebo analgesia involves endogenous opioid peptide release in the vlPAG, we used fiber photometry to measure fluorescence from the genetically encoded opioid sensor δLight.[55] By transducing *Oprm1-Cre* mice,[56] sensor expression was restricted to vlPAG$^{Oprm1\text{-}Cre}$ neurons, which are the most likely targets of endogenous opioid signaling (Figure 4A). Prior to conditioning, placement on the hot plate caused a sustained reduction in sensor fluorescence, which could reflect either an acute loss of opioid tone or, more likely, sensor quenching due to activity-dependent acidification near the plasma membrane in sensor-expressing neurons[57] (Figures 4B and 4C). By contrast, in placebo trials, sensor fluorescence rapidly increased over the first 5 s of noxious stimulus exposure and remained elevated over baseline for at least 10 s thereafter. This finding suggests that placebo conditioning increases noxious stimulus-driven endogenous opioid peptide signaling in the vlPAG.

To determine if vlPAG opioid signaling is necessary for placebo antinociception, we implemented a novel photopharmacological approach involving bilateral photoactivation of photoactivatable naloxone (PhNX), a photo-caged, blood-brain-barrier-permeable derivative of the opioid antagonist naloxone[58] (Figures 4D and 4E). This approach was imperative, as bilateral cannulation lesions much of the PAG, and the excessive animal handling required for drug infusion interferes with placebo conditioning. Further confirming PhNX's inactivity at opioid receptors *in vivo*, systemic PhNX administration (30 mg/kg i.p.) did not attenuate morphine (5 mg/kg i.p.) antinociception in the hot plate assay in the absence of illumination (Figures S4A and S4B). We first determined that bilateral vlPAG illumination with brief 375 nm light flashes (10 × 200 ms, 1 Hz, 22.5 mW) either 2 min before (early) or 37 min after (late) administration of morphine (5 mg/kg i.p.) strongly attenuated the resulting antinociception (Figures 4F and 4G). Notably, early and late naloxone photorelease produced similar effects, indicating that opioid signaling in the vlPAG is necessary for maximal morphine antinociception.

Next, we bilaterally photoreleased naloxone on the placebo test day (Figure 4H). Importantly, PhNX had no effect on placebo antinociception in the absence of illumination (Figures S4C–S4F). To limit our manipulation to a time window involving the noxious stimulus, we photoactivated PhNX (30 mg/kg i.p.) 27 min after placing mice in the morphine-paired chamber, just 3 min prior to hot plate exposure. In comparison to treatment with light and saline, PhNX photoactivation in the vlPAG completely blocked the placebo effect (Figures 4I, 4J, and S4G). These results establish the vlPAG as a critical site of endogenous opioid signaling during the pain-processing phase of placebo pain relief.

Placebo generalization and preventative conditioning for pain resilience

A remarkable feature of placebo analgesia observed in humans is its generality. Encouraged by our findings that conditioning based on paw withdrawals also reduced unconditioned escape behavior (Figures 2P–2R), we wondered if placebo analgesia in mice might also be prone to generalization across pain modalities. We first established that [morphine + noxious stimulus] contextual conditioning was able to produce placebo antinociception using a pinprick assay of mechanical pain sensitivity during conditioning (Figure 5A). On test day, half of the mice in each cohort received saline (placebo), and the other half received naloxone. [Morphine + pinprick] conditioning produced a similar degree of placebo antinociception to that obtained in a parallel group of mice using [morphine + hot plate] conditioning (pinprick: 43.5% ± 10.83% vs. hot plate: 41.36% ± 5.23% of the morphine effect; n = 8 mice per condition, Welch's t test p = 0.86; Figures 5B and 5C). Naloxone completely prevented the placebo effect, indicating that mechanical placebo antinociception is also dependent on endogenous opioid signaling.

Having established that [morphine + noxious stimulus] contextual conditioning can produce placebo antinociception using two distinct pain modalities (thermal and mechanical), we next asked if placebo effects transfer between pain modalities, such that conditioning with a thermal noxious stimulus would generalize to yield antinociception in response to a mechanical noxious stimulus, and vice versa. We first explored a "relay" structure, in which placebo antinociception was initially evoked using the same noxious heat assay (hot plate) used during conditioning and then immediately evaluated using a second noxious mechanical assay (pin prick) in the same context. As shown in Figures 5D, 5E, and S5A, immediately after exhibiting thermal placebo analgesia in response to [morphine + hot plate] conditioning, mice showed a marked reduction in responsivity to the pinprick test as well. Strikingly, the hot plate→pinprick relay placebo effect matches that observed with [morphine + pinprick] conditioning (hot plate→pinprick relay: 67.5% ± 3.1% vs. pinprick conditioning: 70% ± 3.3% of the morphine effect, n = 8 mice per condition, Welch's t test p = 0.59). We found that the placebo relay effect transferred in the other direction as well (Figures 5F, 5G, and S5B). Evoking placebo with the pinprick test after [morphine + pinprick] conditioning reduced thermal sensitivity on a subsequent hot plate test, albeit to a lesser degree than that observed in a group of mice using [morphine + hot plate] conditioning (pinprick→hot plate relay: 8.1 ± 0.8 s vs. hot plate conditioning: 9.8 ± 0.6 s, n = 8 mice per condition, Welch's t test p = 0.11). In both cases, the placebo effect was blocked by naloxone. Conditioning-free control experiments revealed a lack of interaction between the two pain assays (Figures S5C and S5D).

We next asked if placebo antinociception would also transfer across pain modalities in a "substitution" structure, in which one was simply substituted for the other on test day. Similar to the relay scenario, we observed reduced mechanical pain sensitivity when substituting the pinprick test for the hot plate test after [morphine + hot plate] conditioning. The substitution placebo effect on pinprick responsivity was similar to the effect of [morphine + pinprick] conditioning (hot plate→pinprick substitution: 77.5% ± 5.3% vs. pinprick conditioning: 70% ± 3.3% response to pinprick, n = 8 mice per condition, Welch's t test p = 0.25; Figures 5H, 5I, and S5E). This was also the case when substituting the hot plate test for the pinprick test (pinprick→hot plate substitution: 9.62 ± 0.9 s vs. hot plate conditioning: 9.8 ±

Please cite this article in press as: Livrizzi et al., Top-down control of the descending pain modulatory system drives multimodal placebo analgesia, Neuron (2026), https://doi.org/10.1016/j.neuron.2026.03.025

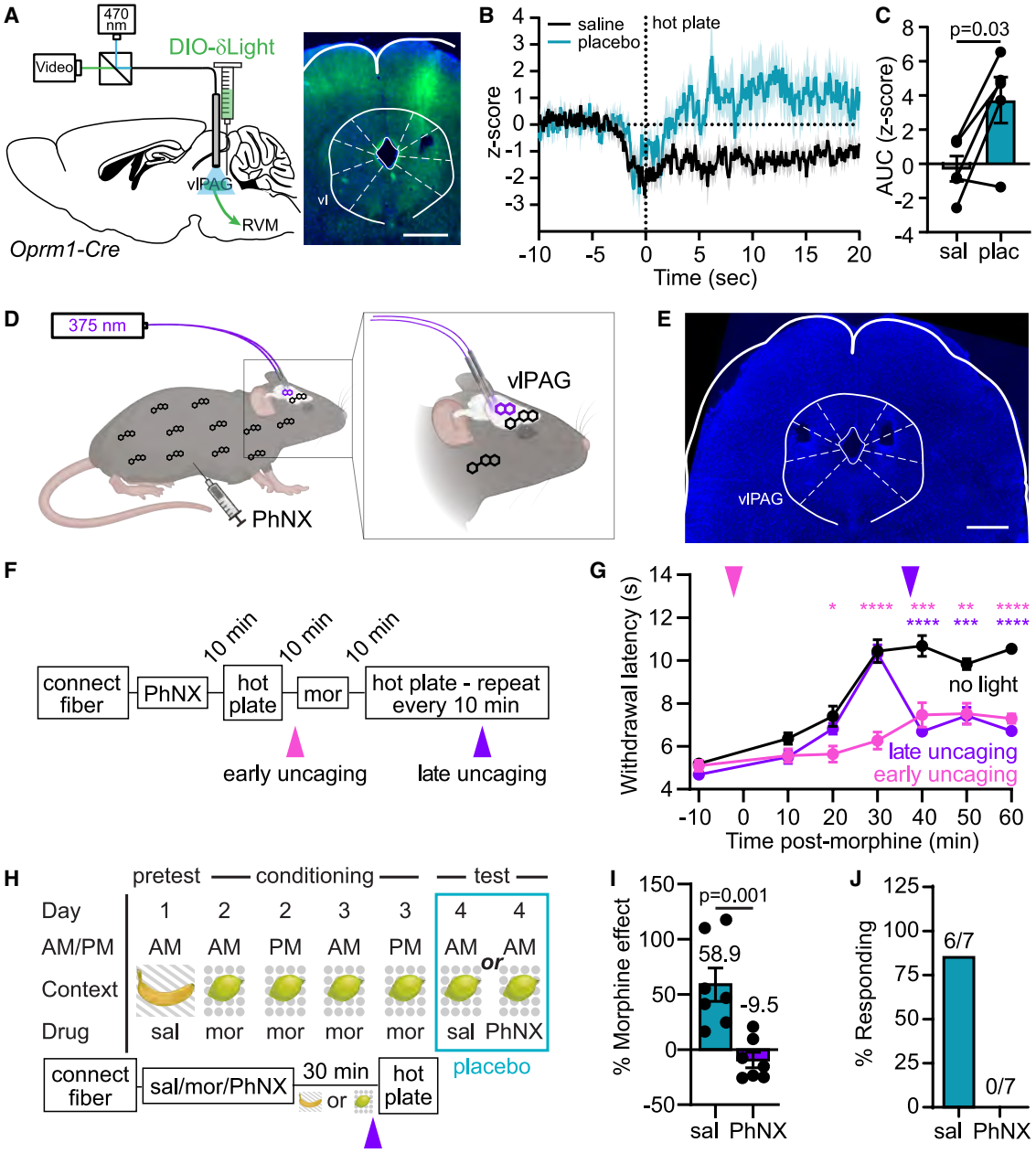

Figure 4. vlPAG opioid signaling underlies morphine and placebo antinociception

(A) Illustration of the viral injection approach for fiber photometry recordings of endogenous opioid peptide signaling from vlPAG$^{Oprm1\text{-}Cre}$ neurons (left) and example of deltaLight expression under the implanted optical fiber (right, scale bar, 500 μm).

(B) Average z-score of opioid peptide activity in vlPAG$^{Oprm1\text{-}Cre}$ neurons upon exposure to the hot plate before and after conditioning (protocol 2, $n = 5$).

(C) Quantification of the opioid activity shown in (B) (integration window: 3 to 8 s, paired t test).

(D) Illustration of the configuration used for bilateral *in vivo* photorelease of naloxone from the caged opioid antagonist PhNX in the vlPAG.

(E) Example of bilateral optical fiber implantation over the vlPAG (scale bar 1 mm).

(F) Timeline for temporally defined *in vivo* naloxone photorelease during morphine analgesia.

(G) Time-course of hot plate withdrawal latencies in response to morphine (5 mg/kg i.p.) and PhNX (30 mg/kg i.p.) administration with light applied in the vlPAG as indicated (no light: $n = 11$, early: $n = 10$, late: $n = 10$, two-way repeated measures ANOVA with Dunnett's post hoc, time × condition $F(12,168) = 13.54$, $p < 0.001$, asterisks are color coded for early and late uncaging compared with the no light condition, $^{*}p < 0.05$, $^{**}p < 0.01$, $^{***}p < 0.001$, $^{****}p < 0.0001$).

(H) Schematic of placebo protocol 2 modified for *in vivo* PhNX photoactivation 3 min prior to hot plate presentation on placebo test day.

(I) Placebo effect quantified as % of the response to the previous dose of morphine upon naloxone photorelease in the vlPAG vs. saline control (saline: $n = 7$, PhNX: $n = 7$, unpaired t test).

(J) Placebo response in (I) was quantified as the % of subjects exhibiting antinociception.

Please cite this article in press as: Livrizzi et al., Top-down control of the descending pain modulatory system drives multimodal placebo analgesia, Neuron (2026), https://doi.org/10.1016/j.neuron.2026.03.025

CellPress
OPEN ACCESS

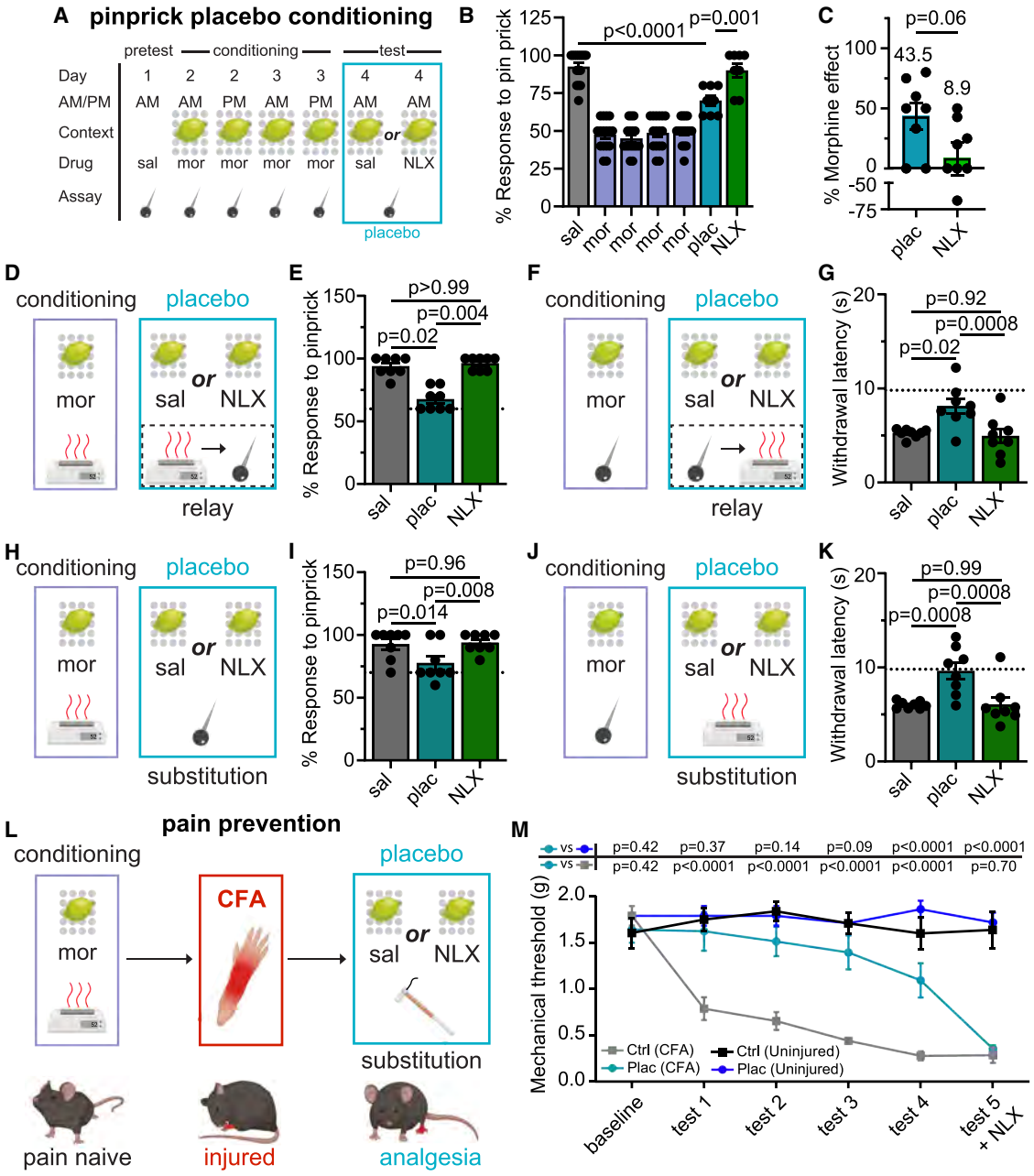

Figure 5. Placebo antinociception generalizes across pain modalities and mitigates injury-induced allodynia

(A) Schematic of the pinprick placebo conditioning protocol.

(B) Responses measured as number of withdrawals to 10 pinpricks applied before, during, and after conditioning ($n = 16$ mice total, placebo: $n = 8$, nlx: $n = 8$, one-way ANOVA, with Sidak's post hoc, $F(6,89) = 56.93$, $p < 0.0001$).

(C) Placebo effect quantified as % of the response to the previous dose of morphine (placebo: $n = 8$, naloxone: $n = 8$, Mann-Whitney test).

(D) Abbreviated schematic of the hot plate→pinprick relay conditioning protocol.

(E) Pinprick responses measured before (sal) and immediately after (plac, NLX) induction of placebo antinociception on the hot plate. A detailed schematic and the hot plate data are shown in Figure S5A ($n = 8$, Friedman test, $H = 14.00$, $p = 0.0003$ with Dunn's post hoc). The dotted line indicates the average % response to pinprick across placebo trials from Figure S5B (60%).

(F) Abbreviated schematic of the pinprick→hot plate relay conditioning protocol.

(G) Paw withdrawal latencies measured before (sal) and immediately after (plac, NLX) induction of placebo antinociception in the pinprick assay. A detailed schematic and the pinprick conditioning data are shown in Figure S5B ($n = 8$, RM one-way ANOVA with Tukey's post hoc, $F(1.586,11.10) = 12.86$, $p = 0.0019$). The dotted line indicates average hot plate withdrawal latency across placebo trials in Figure S5A (9.8 s).

(H) Abbreviated schematic of the hot plate→pinprick substitution conditioning protocol.

(legend continued on next page)

Please cite this article in press as: Livrizzi et al., Top-down control of the descending pain modulatory system drives multimodal placebo analgesia, Neuron (2026), https://doi.org/10.1016/j.neuron.2026.03.025

0.6 s latency, $n = 8$ mice per condition, Welch's t test $p = 0.87$; Figures 5J, 5K, and S5F**)**. All placebo effects were blocked by naloxone. This striking cross-modal generalization of placebo antinociception points to contextual conditioning with analgesics as a potential avenue for inducing broad, modality-independent pain relief.

To investigate whether the generalization of placebo analgesia can be leveraged for pain prevention, we asked whether placebo antinociception induced in a pain-naive state would transfer across both pain state and pain modality to reduce inflammatory mechanical allodynia. We designed a pain-prevention protocol that involved conditioning pain-naive mice and then evaluating placebo antinociception after inducing inflammatory pain with complete Freund's adjuvant (CFA). Following [morphine + hot plate] conditioning, CFA was injected into the left hind paw, and mechanical pain sensitivity was monitored for several days with von Frey fibers (Figures 5L and S5G–S5J). As controls, we used an unpaired conditioning protocol and monitored the uninjured paw in CFA-treated mice. Remarkably, mice that underwent [morphine + hot plate] conditioning exhibited a dramatic reduction in CFA-induced mechanical hypersensitivity compared with mice exposed to the unpaired protocol (Figure 5M). This antinociceptive effect was persistent: over the first 3 days post-CFA, the placebo group showed only minimal mechanical sensitization in the CFA-treated paw relative to the untreated paw. Consistent with a critical role for endogenous opioids, naloxone administration abolished the placebo effect, equalizing mechanical thresholds between CFA-treated paws in both groups. Together, these results demonstrate that placebo conditioning in pain-naive mice can produce long-lasting, cross-modal antinociception after injury, revealing a potential strategy for promoting preventative pain resilience.

DISCUSSION

Using a reverse-translated morphine conditioning paradigm, we show that contextual cues can elicit robust and durable placebo analgesia in mice that shares key features with placebo analgesia in humans.[59,60] Beyond establishing a behavioral model, our findings define a circuit mechanism for placebo analgesia: placebo expression requires engagement of the vlPAG-centered descending pain modulatory pathway and endogenous opioid signaling, and it uniquely depends on top-down cortical inputs from the mPFC and ACC to the PAG. Together with the observation that the placebo antinociception generalizes across distinct pain assays and extends to pain-motivated escape behavior, these results provide a mechanistic framework linking learning, cortical control, and brainstem-mediated descending modulation to placebo pain relief.

A notable feature of the [morphine + noxious stimulus]-conditioned placebo effect in mice is its persistence. Similar to placebo analgesia in humans, the placebo effect was sustained across multiple trials within a session and across sessions over days, with slow and incomplete extinction. In addition, the response was fully restored by reconditioning. This temporal profile is consistent with competing influences that are inherent to placebo analgesia: the omission of the drug should drive extinction, whereas the experience of pain relief can reinforce the conditioned response. The magnitude of placebo analgesia (approximately 30%–60% of the morphine effect) aligns with a human study using a closely related conditioning protocol.[4] Also consistent with many forms of placebo analgesia in humans,[61–63] the placebo effect in this paradigm depends on endogenous opioid neuropeptide signaling. Furthermore, we observed stronger placebo antinociception in pain-naive male mice, mirroring reports from experimental human pain studies in healthy subjects in which males show more frequent or stronger placebo responses under certain induction procedures.[45,64] By contrast, some clinical studies in chronic pain report larger placebo effects in women,[65] highlighting the likelihood that pain state and injury-related plasticity interact with sex to shape placebo responsiveness. Determining how sex differences[66,67] and injury-dependent changes[68,69] in pain modulatory circuitry influence placebo analgesia will be an important direction for future work.

At the circuit level, our results support a central role for the descending pathway in placebo analgesia and identify a specific anatomical route by which prefrontal circuits can exert top-down control over nociceptive processing. The vlPAG is a canonical hub for opioid-mediated descending analgesia, exerting inhibitory control over spinal nociceptive processing via projections to the RVM and the locus coeruleus.[26–30] Although opioids are thought to recruit vlPAG→RVM neurons through disinhibition,[31,32] whether a similar circuit mechanism contributes to placebo analgesia has remained debated.[20–25] Here, we show that morphine antinociception and [morphine + noxious stimulus]-conditioned placebo antinociception converge on vlPAG-dependent mechanisms but diverge in their upstream control: cortical input to the PAG is selectively required for the placebo effect. This placebo-specific dependence on ACC→PAG and mPFC→PAG pathways provides a circuit basis for prior correlational evidence implicating prefrontal regions[70,71] and measures of PFC-PAG and ACC-PAG connectivity[11,12,17] in placebo responsiveness.

These findings also help organize an emerging literature on placebo-like pain relief in rodents, which likely reflects multiple

(I) Same as (E), but for (H), a detailed schematic and the hot plate data are shown in Figure S5E ($n = 8$, RM one-way ANOVA with Tukey's post hoc, $F(2,14) = 7.906$, $p = 0.0050$). The dotted line indicates the average % response to pinprick during the placebo trial in (B) (70%).
(J) Abbreviated schematic of the pinprick→hot plate substitution conditioning protocol.
(K) Same as (G), but for (J). A detailed schematic and the pinprick data are shown in Figure S5F ($n = 8$, RM one-way ANOVA with Tukey's post hoc, $F(2,14) = 15.20$).
(L) Abbreviated schematic of the hot plate→CFA→von Frey pain-prevention conditioning protocol.
(M) Von Frey mechanical thresholds were measured before (baseline) and after (tests 1–5) conditioning on the hot plate and subsequent CFA treatment, and hot plate data are shown in Figures S5G–S5I, and individual von Frey data are shown in Figure S5J ($n = 16$ mice total, placebo: $n = 8$, unpaired: $n = 8$, two-way ANOVA, paired/unpaired vs. CFA interaction: $F(15,140) = 6.442$, $p < 0.0001$, uncorrected Fisher's least significant difference [LSD] post hoc).

Please cite this article in press as: Livrizzi et al., Top-down control of the descending pain modulatory system drives multimodal placebo analgesia, Neuron (2026), https://doi.org/10.1016/j.neuron.2026.03.025

CellPress
OPEN ACCESS

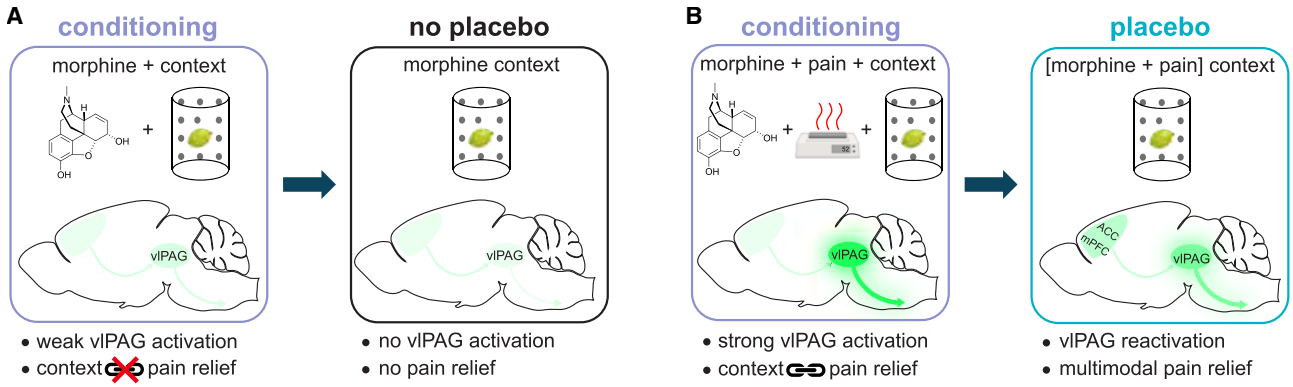

Figure 6. Pavlovian model of contextual conditioning with morphine and pain to produce placebo analgesia

(A) Pairing morphine with context alone during conditioning does not sufficiently engage the descending vlPAG pathway to yield strong reactivation in the morphine context.

(B) By contrast, noxious sensory stimuli strongly activate the descending vlPAG pathway in the presence of morphine such that context becomes associated with pain suppression during conditioning. Subsequently, the [morphine + pain]-conditioned context reactivates the descending pain modulatory pathway via cortical input to the vlPAG.

mechanistic routes. For example, a recent mouse study identified ACC projections to pontine nuclei as critical for a transient conditioned placebo effect that did not rely on opioid drugs. Although opioid blockade abolished the placebo effect, PAG mechanisms were not examined.[72] In a neuropathic pain context, conditioning with gabapentin implicated PFC→PAG neurons as necessary for placebo antinociception, but a causal contribution of endogenous opioids was not established.[73] More broadly, placebo-like analgesia can also be induced using optogenetic activation of pain-suppressing neurons in the central amygdala as an unconditioned stimulus.[74] Against this backdrop, our study delineates an opioid-dependent PAG/descending pathway mechanism for contextual placebo analgesia and provides an explicit, testable framework for evaluating which components are shared across rodent paradigms and which are model-specific.

Our behavioral and circuit results further constrain the learning processes that generate placebo analgesia in this paradigm. Contextual conditioning with morphine alone, in the absence of noxious stimulation (the unpaired protocol), was insufficient to produce antinociception in the morphine-paired context (Figure 6A). This requirement for pairing analgesia with a noxious stimulus suggests that conditioned placebo analgesia is not simply a context-evoked opioid state but instead depends on learning that links contextual cues to an altered expected experience of the aversive stimulus. The opioid dependence of the placebo effect is consistent with an expectation-dependent process[4,75] and aligns with predictive coding accounts in which descending control tunes ascending sensory input toward learned predictions about noxious stimuli.[3,76] In this context, the TRAP experiments provide evidence consistent with Pavlovian associative plasticity (Figure 6B): conditioning enables the context (conditioned stimulus) to recruit pain-suppressing descending pathway activity that is normally engaged by the combined unconditioned stimulus of morphine and noxious stimulation during training. Because TRAP labeling was performed in the conditioned context without noxious stimulation, the labeled vlPAG (and upstream) neurons represent context-activated ensembles. Their projection to the RVM and the antinociception produced by their chemogenetic reactivation indicate that contextual cues alone can engage descending pathway circuitry sufficient to place animals in a hypoalgesic state.

An additional primary outcome is that conditioned analgesia generalized beyond the specific training conditions. Placebo pain relief transferred across distinct pain assays in substitution designs (e.g., analgesia on pinprick after [morphine + hot plate] conditioning and vice versa) and within a given assay extended to unconditioned pain-related behavior (escape from the hot plate). These results increase the translational relevance of rodent placebo models to clinical contexts, in which patients' prior experiences with drugs and treatment settings can generalize to broader expectations of improvement.[35,36,77] Notably, cross-assay transfer was not an *a priori* expectation. From a predictive coding perspective, animals were not trained to predict the intensity of the unconditioned noxious stimulus. Furthermore, descending pathway architecture includes modality-selective components—for example, enkephalinergic RVM→dorsal horn neurons suppress mechanical but not thermal nociception, suggesting parallel descending pathways with different modality tuning.[78] The observation of cross-assay placebo antinociception therefore motivates the hypothesis that convergence occurs at upstream descending pathway nodes such as the vlPAG, where pharmacological[79,80] and chemogenetic[34] manipulations can bidirectionally influence multiple pain modalities.

Finally, the generality of conditioned placebo analgesia carries translational implications. Placebo antinociception transferred not only across pain assays but also across pain states: conditioning in pain-naive animals reduced mechanical hypersensitivity after inflammatory insult. This breadth suggests a potential strategy for preemptive conditioning to build resilience to pain associated with future injury.[81] In a clinical setting, such an approach could be incorporated into preparatory regimens to reduce pain after planned medical procedures, including surgery. Translation will require conditioning protocols that use

Please cite this article in press as: Livrizzi et al., Top-down control of the descending pain modulatory system drives multimodal placebo analgesia, Neuron (2026), https://doi.org/10.1016/j.neuron.2026.03.025

non-opioid analgesics and noxious stimuli that are tolerable and ethically appropriate, as well as careful delineation of the boundary conditions under which generalized placebo analgesia is expressed. It will also be important to determine how broadly cross-assay placebo analgesia extends across clinically relevant pain states, including neuropathic and chronic pain. Bridging clinical and pre-clinical paradigms for the study of cognitive pain modulation holds great promise for uncovering mechanistic insights that will inform more effective and durable approaches to the treatment of pain.

RESOURCE AVAILABILITY

Lead contact

Requests for further information or resources should be addressed to and will be fulfilled by the lead contact, Dr. Matthew R. Banghart (mbanghart@ucsd.edu).

Materials availability

This study did not generate any new materials.

Data and code availability

All data shown in the figures are available in the source data file within the supporting information. This paper does not report original code.

ACKNOWLEDGMENTS

The authors thank M. Smith, Y. Aljadeff, F. Zeidan, T. Yaksh, Y. Shaham, and members of the Banghart Laboratory for helpful discussions; B. Stepanyuk and E. Berg for AAV production; and W.S. Song and Y. Kim for artwork. Figures 1, 4, 5, and 6 were partially created with BioRender.com. This work was supported by the Rita Allen Foundation (M.R.B.), the Esther A. & Joseph Klingenstein Fund and Simons Foundation (M.R.B.), the Brain & Behavior Research Foundation (M.R.B.), R00DA034648 (M.R.B.), RF1NS126073 (M.R.B.), U01NS113295 (M.R.B. and L.T.) including a BRAIN Initiative Diversity Supplement (D.A.J.), U01NS120820 (L.T.), UM1MH136462 (L.T.), DP2GM140923 (G.C.), R01DA056581 (K.T.B.), R01DA056599 (G.C. and K.T.B.), K99DA060979 (B.A.K.), and T32GM133351 (J.C.-W.).

AUTHOR CONTRIBUTIONS

G.L., S.T.L., and M.R.B. conceived the project. G.L., J.C.-W., D.A.J., S.T.L., and J.L. designed and performed most of the experiments. C.D. and L.T. generated, characterized, and provided δLight. B.A.K. performed the TRAP experiments under the supervision of G.C. Y.L. performed the RABV experiments under the supervision of K.T.B. G.L., J.C.-W., and M.R.B. wrote the manuscript. All authors interpreted the data, contributed to data analysis, and discussed the manuscript. M.R.B. supervised the project.

DECLARATION OF INTERESTS

The authors declare no competing interests.

STAR★METHODS

Detailed methods are provided in the online version of this paper and include the following:

- KEY RESOURCES TABLE
- EXPERIMENTAL MODEL AND STUDY PARTICIPANT DETAILS
  - Animals
- METHOD DETAILS
  - Drugs
  - Viral constructs
  - Surgery
  - Chemogenetic manipulation
  - Pain behavior assessment
  - Hot Plate Test
  - Von Frey Test
  - Pinprick Test
  - Hot Plate Placebo Conditioning
  - Pinprick Placebo Conditioning
  - Pain Modality Transfer Experiments
  - Fiber photometry
  - *In vivo* drug uncaging
  - RABV monosynaptic tracing
  - RABV Mapping
  - Histology
  - Statistics

SUPPLEMENTAL INFORMATION

Supplemental information can be found online at https://doi.org/10.1016/j.neuron.2026.03.025.

Received: September 10, 2024
Revised: January 12, 2026
Accepted: March 18, 2026

REFERENCES

1. Wager, T.D., and Atlas, L.Y. (2015). The neuroscience of placebo effects: Connecting context, learning and health. Nat. Rev. Neurosci. *16*, 403–418. https://doi.org/10.1038/nrn3976.
2. Benedetti, F. (2014). Placebo effects: From the neurobiological paradigm to translational implications. Neuron *84*, 623–637. https://doi.org/10.1016/j.neuron.2014.10.023.
3. Büchel, C., Geuter, S., Sprenger, C., and Eippert, F. (2014). Placebo Analgesia: A Predictive Coding Perspective. Neuron *81*, 1223–1239. https://doi.org/10.1016/j.neuron.2014.02.042.
4. Amanzio, M., and Benedetti, F. (1999). Neuropharmacological dissection of placebo analgesia: Expectation- activated opioid systems versus conditioning-activated specific subsystems. J. Neurosci. *19*, 484–494. https://doi.org/10.1523/jneurosci.19-01-00484.1999.
5. Enck, P., Bingel, U., Schedlowski, M., and Rief, W. (2013). The placebo response in medicine: Minimize, maximize or personalize? Nat. Rev. Drug Discov. *12*, 191–204. https://doi.org/10.1038/nrd3923.
6. Tuttle, A.H., Tohyama, S., Ramsay, T., Kimmelman, J., Schweinhardt, P., Bennett, G.J., and Mogil, J.S. (2015). Increasing placebo responses over time in U.S. clinical trials of neuropathic pain. Pain *156*, 2616–2626. https://doi.org/10.1097/j.pain.0000000000000333.
7. Colloca, L., Enck, P., and Degrazia, D. (2016). Relieving pain using dose-extending placebos: A scoping review. Pain *157*, 1590–1598. https://doi.org/10.1097/j.pain.0000000000000566.
8. Darnall, B.D., and Colloca, L. (2018). Optimizing Placebo and Minimizing Nocebo to Reduce Pain, Catastrophizing, and Opioid Use: A Review of the Science and an Evidence-Informed Clinical Toolkit. Int. Rev. Neurobiol. *139*, 129–157. https://doi.org/10.1016/bs.irn.2018.07.022.
9. Wager, T.D., Rilling, J.K., Smith, E.E., Sokolik, A., Casey, K.L., Davidson, R.J., Kosslyn, S.M., Rose, R.M., and Cohen, J.D. (2004). Placebo-Induced Changes in fMRI in the Anticipation and Experience of Pain. Science *303*, 1162–1167. https://doi.org/10.1126/science.1093065.
10. Eippert, F., Bingel, U., Schoell, E.D., Yacubian, J., Klinger, R., Lorenz, J., and Büchel, C. (2009). Activation of the Opioidergic Descending Pain Control System Underlies Placebo Analgesia. Neuron *63*, 533–543. https://doi.org/10.1016/j.neuron.2009.07.014.
11. Bingel, U., Lorenz, J., Schoell, E., Weiller, C., and Büchel, C. (2006). Mechanisms of placebo analgesia: rACC recruitment of a subcortical

Please cite this article in press as: Livrizzi et al., Top-down control of the descending pain modulatory system drives multimodal placebo analgesia, Neuron (2026), https://doi.org/10.1016/j.neuron.2026.03.025

CellPress
OPEN ACCESS

antinociceptive network. Pain *120*, 8–15. https://doi.org/10.1016/j.pain.2005.08.027.

12. Stein, N., Sprenger, C., Scholz, J., Wiech, K., and Bingel, U. (2012). White matter integrity of the descending pain modulatory system is associated with interindividual differences in placebo analgesia. Pain *153*, 2210–2217. https://doi.org/10.1016/j.pain.2012.07.010.
13. Levine, J.D., Gordon, N.C., and Fields, H.L. (1978). THE MECHANISM OF PLACEBO ANALGESIA. Lancet *2*, 654–657. https://doi.org/10.1016/S0140-6736(78)92762-9.
14. Guo, J.Y., Wang, J.Y., and Luo, F. (2010). Dissection of placebo analgesia in mice: The conditions for activation of opioid and non-opioid systems. J. Psychopharmacol. *24*, 1561–1567. https://doi.org/10.1177/0269881109104848.
15. Wager, T.D., Scott, D.J., and Zubieta, J.K. (2007). Placebo effects on human μ-opioid activity during pain. Proc. Natl. Acad. Sci. USA *104*, 11056–11061. https://doi.org/10.1073/pnas.0702413104.
16. Zubieta, J.K., Bueller, J.A., Jackson, L.R., Scott, D.J., Xu, Y., Koeppe, R.A., Nichols, T.E., and Stohler, C.S. (2005). Placebo effects mediated by endogenous opioid activity on μ-opioid receptors. J. Neurosci. *25*, 7754–7762. https://doi.org/10.1523/JNEUROSCI.0439-05.2005.
17. Petrovic, P., Kalso, E., Petersson, K.M., and Ingvar, M. (2002). Placebo and Opioid Analgesia– Imaging a Shared Neuronal Network. Science *295*, 1737–1740. https://doi.org/10.1126/science.1067176.
18. Eippert, F., Finsterbusch, J., Bingel, U., and Büchel, C. (2009). Direct evidence for spinal cord involvement in Placebo Analgesia. Science *326*, 404. https://doi.org/10.1126/science.1180142.
19. Tracey, I. (2010). Getting the pain you expect: Mechanisms of placebo, nocebo and reappraisal effects in humans. Nat. Med. *16*, 1277–1283. https://doi.org/10.1038/nm.2229.
20. Botvinik-Nezer, R., Petre, B., Ceko, M., Lindquist, M.A., Friedman, N.P., and Wager, T.D. (2024). Placebo treatment affects brain systems related to affective and cognitive processes, but not nociceptive pain. Nat. Commun. *15*, 6017. https://doi.org/10.1038/s41467-024-50103-8.
21. Wager, T.D., Matre, D., and Casey, K.L. (2006). Placebo effects in laser-evoked pain potentials. Brain Behav. Immun. *20*, 219–230. https://doi.org/10.1016/j.bbi.2006.01.007.
22. Woo, C.W., Roy, M., Buhle, J.T., and Wager, T.D. (2015). Distinct Brain Systems Mediate the Effects of Nociceptive Input and Self-Regulation on Pain. PLoS Biol. *13*, e1002036. https://doi.org/10.1371/journal.pbio.1002036.
23. Martini, M., Lee, M.C.H., Valentini, E., and Iannetti, G.D. (2015). Intracortical modulation, and not spinal inhibition, mediates placebo analgesia. Eur. J. Neurosci. *41*, 498–504. https://doi.org/10.1111/ejn.12807.
24. DosSantos, M.F., Martikainen, I.K., Nascimento, T.D., Love, T.M., DeBoer, M.D., Schambra, H.M., Bikson, M., Zubieta, J.K., and DaSilva, A.F. (2014). Building up analgesia in humans via the endogenous μ-opioid system by combining placebo and active tDCS: A preliminary report. PLoS One *9*, e102350. https://doi.org/10.1371/journal.pone.0102350.
25. Scott, D.J., Stohler, C.S., Egnatuk, C.M., Wang, H., Koeppe, R.A., and Zubieta, J.K. (2008). Placebo and nocebo effects are defined by opposite opioid and dopaminergic responses. Arch. Gen. Psychiatry *65*, 220–231. https://doi.org/10.1001/archgenpsychiatry.2007.34.
26. Basbaum, A.I., Marley, N.J.E., O'Keefe, J., and Clanton, C.H. (1977). Reversal of morphine and stimulus-produced analgesia by subtotal spinal cord lesions. Pain *3*, 43–56. https://doi.org/10.1016/0304-3959(77)90034-3.
27. Liebeskind, J.C., Guilbaud, G., Besson, J.M., and Oliveras, J.L. (1973). Analgesia from electrical stimulation of the periaqueductal gray matter in the cat: behavioral observations and inhibitory effects on spinal cord interneurons. Brain Res. *50*, 441–446. https://doi.org/10.1016/0006-8993(73)90748-8.
28. Yaksh, T.L., Yeung, J.C., and Rudy, T.A. (1976). Systematic examination in the rat of brain sites sensitive to the direct application of morphine: observation of differential effects within the periaqueductal gray. Brain Res. *114*, 83–103. https://doi.org/10.1016/0006-8993(76)91009-X.
29. Fields, H. (2004). State-dependent opioid control of pain. Nat. Rev. Neurosci. *5*, 565–575. https://doi.org/10.1038/nrn1431.
30. Lubejko, S.T., Livrizzi, G., Buczynski, S.A., Patel, J., Yung, J.C., Yaksh, T.L., and Banghart, M.R. (2024). Inputs to the locus coeruleus from the periaqueductal gray and rostroventral medulla shape opioid-mediated descending pain modulation. Sci. Adv. *10*, eadj9581. https://doi.org/10.1126/SCIADV.ADJ9581.
31. Moreau, J.L., and Fields, H.L. (1986). Evidence for GABA involvement in midbrain control of medullary neurons that modulate nociceptive transmission. Brain Res. *397*, 37–46. https://doi.org/10.1016/0006-8993(86)91367-3.
32. Basbaum, A.I., and Fields, H.L. (1984). Endogenous Pain Control Systems: Brainstem Spinal Pathways and Endorphin Circuitry. Annu. Rev. Neurosci. *7*, 309–338. https://doi.org/10.1146/annurev.ne.07.030184.001521.
33. Tovote, P., Esposito, M.S., Botta, P., Chaudun, F., Fadok, J.P., Markovic, M., Wolff, S.B.E., Ramakrishnan, C., Fenno, L., Deisseroth, K., et al. (2016). Midbrain circuits for defensive behaviour. Nature *534*, 206–212. https://doi.org/10.1038/nature17996.
34. Samineni, V.K., Grajales-Reyes, J.G., Copits, B.A., O'Brien, D.E., Trigg, S.L., Gomez, A.M., Bruchas, M.R., and Gereau, R.W. (2017). Divergent modulation of nociception by glutamatergic and GABAergic neuronal subpopulations in the periaqueductal gray. eNeuro *4*. ENEURO.0129-16.2017. https://doi.org/10.1523/ENEURO.0129-16.2017.
35. Klinger, R., Colloca, L., Bingel, U., and Flor, H. (2014). Placebo analgesia: Clinical applications. Pain *155*, 1055–1058. https://doi.org/10.1016/j.pain.2013.12.007.
36. Bouhassira, D. (2026). Placebo Responses in Clinical Trials of Analgesics. Neurol. Clin. *44*, 11–22. https://doi.org/10.1016/j.ncl.2025.08.002.
37. Weng, L., Peerdeman, K.J., Della Porta, D., Van Laarhoven, A.I.M., and Evers, A.W.M. (2022). Can placebo and nocebo effects generalize within pain modalities and across somatosensory sensations? Pain *163*, 548–559. https://doi.org/10.1097/j.pain.0000000000002390.
38. Weng, L., Peerdeman, K.J., van Laarhoven, A.I.M., and Evers, A.W.M. (2025). Generalisation of Placebo and Nocebo Effects: Current Knowledge and Future Directions. Eur. J. Pain *29*, e70018. https://doi.org/10.1002/ejp.70018.
39. Benedetti, F., Pollo, A., and Colloca, L. (2007). Opioid-mediated placebo responses boost pain endurance and physical performance: is it doping in sport competitions? J. Neurosci. *27*, 11934–11939. https://doi.org/10.1523/JNEUROSCI.3330-07.2007.
40. Bryant, C.D., Roberts, K.W., Culbertson, C.S., Le, A., Evans, C.J., and Fanselow, M.S. (2009). Pavlovian conditioning of multiple opioid-like responses in mice. Drug Alcohol Depend. *103*, 74–83. https://doi.org/10.1016/j.drugalcdep.2009.03.016.
41. Keller, A., Akintola, T., and Colloca, L. (2018). Placebo Analgesia in Rodents: Current and Future Research. Int. Rev. Neurobiol. *138*, 1–15. https://doi.org/10.1016/bs.irn.2018.02.001.
42. Miller, J.S., Kelly, K.S., Neisewander, J.L., McCoy, D.F., and Bardo, M.T. (1990). Conditioning of morphine-induced taste aversion and analgesia. Psychopharmacology (Berl.) *101*, 472–480. https://doi.org/10.1007/BF02244224.
43. Nieto, M.M., Wilson, J., Cupo, A., Roques, B.P., and Noble, F. (2002). Chronic Morphine Treatment Modulates the Extracellular Levels of Endogenous Enkephalins in Rat Brain Structures Involved in Opiate Dependence: A Microdialysis Study. J. Neurosci. *22*, 1034–1041. https://doi.org/10.1523/JNEUROSCI.22-03-01034.2002.
44. Valone, J.M., Randall, C.K., Kraemer, P.J., and Bardo, M.T. (1998). Olfactory cues and morphine-induced conditioned analgesia in rats. Pharmacol. Biochem. Behav. *60*, 115–118. https://doi.org/10.1016/S0091-3057(97)00554-6.

Please cite this article in press as: Livrizzi et al., Top-down control of the descending pain modulatory system drives multimodal placebo analgesia, Neuron (2026), https://doi.org/10.1016/j.neuron.2026.03.025

45. Vambheim, S.M., and Flaten, M.A. (2017). A systematic review of sex differences in the placebo and the nocebo effect. J. Pain Res. *10*, 1831–1839. https://doi.org/10.2147/JPR.S134745.

46. Denardo, L.A., Liu, C.D., Allen, W.E., Adams, E.L., Friedmann, D., Fu, L., Guenthner, C.J., Tessier-Lavigne, M., and Luo, L. (2019). Temporal evolution of cortical ensembles promoting remote memory retrieval. Nat. Neurosci. *22*, 460–469. https://doi.org/10.1038/s41593-018-0318-7.

47. Roth, B.L. (2016). DREADDs for Neuroscientists. Neuron *89*, 683–694. https://doi.org/10.1016/j.neuron.2016.01.040.

48. Tervo, D.G.R., Hwang, B.-Y., Viswanathan, S., Gaj, T., Lavzin, M., Ritola, K.D., Lindo, S., Michael, S., Kuleshova, E., Ojala, D., et al. (2016). A Designer AAV Variant Permits Efficient Retrograde Access to Projection Neurons. Neuron *92*, 372–382. https://doi.org/10.1016/j.neuron.2016.09.021.

49. Zhang, Y., Rózsa, M., Liang, Y., Bushey, D., Wei, Z., Zheng, J., Reep, D., Broussard, G.J., Tsang, A., Tsegaye, G., et al. (2023). Fast and sensitive GCaMP calcium indicators for imaging neural populations. Nature *615*, 884–891. https://doi.org/10.1038/s41586-023-05828-9.

50. George, D.T., Ameli, R., and Koob, G.F. (2019). Periaqueductal Gray Sheds Light on Dark Areas of Psychopathology. Trends Neurosci. *42*, 349–360. https://doi.org/10.1016/J.TINS.2019.03.004.

51. Bäck, S., Necarsulmer, J., Whitaker, L.R., Coke, L.M., Koivula, P., Heathward, E.J., Fortuno, L.V., Zhang, Y., Yeh, C.G., Baldwin, H.A., et al. (2019). Neuron-Specific Genome Modification in the Adult Rat Brain Using CRISPR-Cas9 Transgenic Rats. Neuron *102*, 105–119.e8. https://doi.org/10.1016/j.neuron.2019.01.035.

52. Wiech, K., Lin, C.S., Brodersen, K.H., Bingel, U., Ploner, M., and Tracey, I. (2010). Anterior insula integrates information about salience into perceptual decisions about pain. J. Neurosci. *30*, 16324–16331. https://doi.org/10.1523/JNEUROSCI.2087-10.2010.

53. Huang, J., Gadotti, V.M., Chen, L., Souza, I.A., Huang, S., Wang, D., Ramakrishnan, C., Deisseroth, K., Zhang, Z., and Zamponi, G.W. (2019). A neuronal circuit for activating descending modulation of neuropathic pain. Nat. Neurosci. *22*, 1659–1668. https://doi.org/10.1038/s41593-019-0481-5.

54. Tsou, K., and Jang, C.S. (1964). Studies on the site of analgesic action of morphine by intracerebral micro-injection. Sci. Sin. *13*, 1099–1109. https://doi.org/10.1097/00132586-196512000-00023.

55. Dong, C., Gowrishankar, R., Jin, Y., He, X.J., Gupta, A., Wang, H., Sayar-Atasoy, N., Flores, R.J., Mahe, K., Tjahjono, N., et al. (2024). Unlocking opioid neuropeptide dynamics with genetically encoded biosensors. Nat. Neurosci. *27*, 1844–1857. https://doi.org/10.1038/s41593-024-01697-1.

56. Bailly, J., Del Rossi, N., Runtz, L., Li, J.J., Park, D., Scherrer, G., Tanti, A., Birling, M.C., Darcq, E., and Kieffer, B.L. (2020). Targeting morphine-responsive neurons: Generation of a knock-in mouse line expressing cre recombinase from the Mu-opioid receptor gene locus. eNeuro *7*. ENEURO.0433-19.2020. https://doi.org/10.1523/ENEURO.0433-19.2020.

57. Wu, Z., Cui, Y., Wang, H., Wu, H., Wan, Y., Li, B., Wang, L., Pan, S., Peng, W., Dong, A., et al. (2023). Neuronal activity-induced, equilibrative nucleoside transporter-dependent, somatodendritic adenosine release revealed by a GRAB sensor. Proc. Natl. Acad. Sci. USA *120*, e2212387120. https://doi.org/10.1073/pnas.2212387120.

58. McClain, S.P., Ma, X., Johnson, D.A., Johnson, C.A., Layden, A.E., Yung, J.C., Lubejko, S.T., Livrizzi, G., He, X.J., Zhou, J., et al. (2023). In vivo photopharmacology with light-activated opioid drugs. Neuron *111*, 3926–3940.e10. https://doi.org/10.1016/j.neuron.2023.09.017.

59. Colloca, L., and Benedetti, F. (2006). How prior experience shapes placebo analgesia. Pain *124*, 126–133. https://doi.org/10.1016/j.pain.2006.04.005.

60. Schafer, S.M., Geuter, S., and Wager, T.D. (2018). Mechanisms of placebo analgesia: A dual-process model informed by insights from cross-species comparisons. Prog. Neurobiol. *160*, 101–122. https://doi.org/10.1016/j.pneurobio.2017.10.008.

61. Sauro, M.D., and Greenberg, R.P. (2005). Endogenous opiates and the placebo effect: A meta-analytic review. J. Psychosom. Res. *58*, 115–120. https://doi.org/10.1016/j.jpsychores.2004.07.001.

62. ter Riet, G., De Craen, A.J.M., De Boer, A., and Kessels, A.G.H. (1998). Is placebo analgesia mediated by endogenous opioids? A systematic review. Pain *76*, 273–275. https://doi.org/10.1016/S0304-3959(98)00057-8.

63. Saunders, A., Macosko, E.Z., Wysoker, A., Goldman, M., Krienen, F.M., de Rivera, H., Bien, E., Baum, M., Bortolin, L., Wang, S., et al. (2018). Molecular Diversity and Specializations among the Cells of the Adult Mouse Brain. Cell *174*, 1015–1030.e16. https://doi.org/10.1016/J.CELL.2018.07.028.

64. Enck, P., and Klosterhalfen, S. (2019). Does sex/gender play a role in placebo and nocebo effects? Conflicting evidence from clinical trials and experimental studies. Front. Neurosci. *13*, 416027. https://doi.org/10.3389/FNINS.2019.00160/BIBTEX.

65. Olson, E.M., Akintola, T., Phillips, J., Blasini, M., Haycock, N.R., Martinez, P.E., Greenspan, J.D., Dorsey, S.G., Wang, Y., and Colloca, L. (2021). Effects of sex on placebo effects in chronic pain participants: A cross-sectional study. Pain *162*, 531–542. https://doi.org/10.1097/j.pain.0000000000002038.

66. Loyd, D.R., and Murphy, A.Z. (2006). Sex differences in the anatomical and functional organization of the periaqueductal gray-rostral ventromedial medullary pathway in the rat: A potential circuit mediating the sexually dimorphic actions of morphine. J. Comp. Neurol. *496*, 723–738. https://doi.org/10.1002/cne.20962.

67. Averitt, D.L., Eidson, L.N., Doyle, H.H., and Murphy, A.Z. (2019). Neuronal and glial factors contributing to sex differences in opioid modulation of pain. Neuropsychopharmacology *44*, 155–165. https://doi.org/10.1038/s41386-018-0127-4.

68. McPherson, K.B., Bouchet, C.A., Coutens, B., and Ingram, S.L. (2023). Persistent inflammation selectively activates opioid-sensitive phasic-firing neurons within the vlPAG. J. Neurophysiol. *129*, 1237–1248. https://doi.org/10.1152/jn.00016.2023.

69. Tonsfeldt, K.J., Suchland, K.L., Beeson, K.A., Lowe, J.D., Li, M.H., and Ingram, S.L. (2016). Sex differences in GABAA signaling in the periaqueductal gray induced by persistent inflammation. J. Neurosci. *36*, 1669–1681. https://doi.org/10.1523/JNEUROSCI.1928-15.2016.

70. Krummenacher, P., Candia, V., Folkers, G., Schedlowski, M., and Schönbächler, G. (2010). Prefrontal cortex modulates placebo analgesia. Pain *148*, 368–374. https://doi.org/10.1016/j.pain.2009.09.033.

71. Xu, L., Wan, Y., Ma, L., Zheng, J., Han, B., Liu, F.Y., Yi, M., and Wan, Y. (2018). A Context-Based Analgesia Model in Rats: Involvement of Prefrontal Cortex. Neurosci. Bull. *34*, 1047–1057. https://doi.org/10.1007/s12264-018-0279-6.

72. Chen, C., Niehaus, J.K., Dinc, F., Huang, K.L., Barnette, A.L., Tassou, A., Shuster, S.A., Wang, L., Lemire, A., Menon, V., et al. (2024). Neural circuit basis of placebo pain relief. Nature *632*, 1092–1100. https://doi.org/10.1038/S41586-024-07816-Z.

73. Neyama, H., Wu, Y., Nakaya, Y., Kato, S., Shimizu, T., Tahara, T., Shigeta, M., Inoue, M., Miyamichi, K., Matsushita, N., et al. (2025). Opioidergic activation of the descending pain inhibitory system underlies placebo analgesia. Sci. Adv. *11*, eadp8494. https://doi.org/10.1126/SCIADV.ADP8494.

74. Chen, B., Goldstein, N., Dziubek, J., Sundai, A., Zhao, S., Harrahill, A., Choi, S., Prevosto, V., and Wang, F. (2024). Reverse-engineering placebo analgesia. Curr. Biol. *34*, 4261–4271.e5. https://doi.org/10.1016/j.cub.2024.08.004.

75. Benedetti, F., Amanzio, M., Rosato, R., and Blanchard, C. (2011). Nonopioid placebo analgesia is mediated by CB1 cannabinoid receptors. Nat. Med. *17*, 1228–1230. https://doi.org/10.1038/nm.2435.

76. Ozawa, T., Ycu, E.A., Kumar, A., Yeh, L.F., Ahmed, T., Koivumaa, J., and Johansen, J.P. (2017). A feedback neural circuit for calibrating aversive

Please cite this article in press as: Livrizzi et al., Top-down control of the descending pain modulatory system drives multimodal placebo analgesia, Neuron (2026), https://doi.org/10.1016/j.neuron.2026.03.025

memory strength. Nat. Neurosci. *20*, 90–97. https://doi.org/10.1038/nn.4439.

77. Colloca, L., Klinger, R., Flor, H., and Bingel, U. (2013). Placebo analgesia: Psychological and neurobiological mechanisms. Pain *154*, 511–514. https://doi.org/10.1016/j.pain.2013.02.002.

78. François, A., Low, S.A., Sypek, E.I., Christensen, A.J., Sotoudeh, C., Beier, K.T., Ramakrishnan, C., Ritola, K.D., Sharif-Naeini, R., Deisseroth, K., et al. (2017). A Brainstem-Spinal Cord Inhibitory Circuit for Mechanical Pain Modulation by GABA and Enkephalins. Neuron *93*, 822–839.e6. https://doi.org/10.1016/j.neuron.2017.01.008.

79. Tortorici, V., Morgan, M.M., and Vanegas, H. (2001). Tolerance to repeated microinjection of morphine into the periaqueductal gray is associated with changes in the behavior of off- and on-cells in the rostral ventromedial medulla of rats. Pain *89*, 237–244. https://doi.org/10.1016/S0304-3959(00)00367-5.

80. Sohn, J.H., Lee, B.H., Park, S.H., Ryu, J.W., Kim, B.O., and Park, Y.G. (2000). Microinjection of opiates into the periaqueductal gray matter attenuates neuropathic pain symptoms in rats. NeuroReport *11*, 1413–1416. https://doi.org/10.1097/00001756-200005150-00012.

81. Shpaner, M., Kelly, C., Lieberman, G., Perelman, H., Davis, M., Keefe, F.J., and Naylor, M.R. (2014). Unlearning chronic pain: A randomized controlled trial to investigate changes in intrinsic brain connectivity following Cognitive Behavioral Therapy. Neuroimage Clin. *5*, 365–376. https://doi.org/10.1016/j.nicl.2014.07.008.

82. Bruno, C.A., O'Brien, C., Bryant, S., Mejaes, J.I., Estrin, D.J., Pizzano, C., and Barker, D.J. (2021). pMAT: An open-source software suite for the analysis of fiber photometry data. Pharmacol. Biochem. Behav. *201*, 173093. https://doi.org/10.1016/j.pbb.2020.173093.

83. Lopes, G., Bonacchi, N., Frazão, J., Neto, J.P., Atallah, B.V., Soares, S., Moreira, L., Matias, S., Itskov, P.M., Correia, P.A., et al. (2015). Bonsai: an event-based framework for processing and controlling data streams. Front. Neuroinform. *9*, 7. https://doi.org/10.3389/fninf.2015.00007.

84. Chaplan, S.R., Bach, F.W., Pogrel, J.W., Chung, J.M., and Yaksh, T.L. (1994). Quantitative assessment of tactile allodynia in the rat paw. J. Neurosci. Methods *53*, 55–63. https://doi.org/10.1016/0165-0270(94)90144-9.

85. Rosen, S.F., Lima, L.V., Chen, C., Nejade, R., Zhao, M., Nemoto, W., Toprak, E., Skvortsova, A., Tansley, S.N., Zumbusch, A., et al. (2022). Olfactory exposure to late-pregnant and lactating mice causes stress-induced analgesia in male mice. Sci. Adv. *8*, eabi9366. https://doi.org/10.1126/sciadv.abi9366.

86. Corder, G., Doolen, S., Donahue, R.R., Winter, M.K., Jutras, B.L., He, Y., Hu, X., Wieskopf, J.S., Mogil, J.S., Storm, D.R., et al. (2013). Constitutive μ-opioid receptor activity leads to long-term endogenous analgesia and dependence. Science *341*, 1394–1399. https://doi.org/10.1126/science.1239403.

Please cite this article in press as: Livrizzi et al., Top-down control of the descending pain modulatory system drives multimodal placebo analgesia, Neuron (2026), https://doi.org/10.1016/j.neuron.2026.03.025

STAR★METHODS

KEY RESOURCES TABLE

REAGENT or RESOURCE	SOURCE	IDENTIFIER
Antibodies		
Guinea pig anti-cFOS	Synaptic Systems	Cat#226 308; RRID: AB_2905595
Chicken anti-GFP	Abcam	Cat#ab13970; RRID: AB_300798
Rabbit anti-DsRed	Takara Bio	Cat#632496; RRID: AB_10013483
Alexa-Fluor 488 goat anti-guinea pig	Abcam	Cat#150185; RRID: AB_2736871
Alexa-Fluor 488 donkey anti-chicken	Jackson ImmunoResearch	Cat#703-545-155; RRID:AB_2340375
Alexa-Fluor 594 donkey anti-rabbit	Thermo Scientific	Cat#A21207; RRID:AB_141637
Bacterial and virus strains		
AAVretro-pgk-Cre	Addgene	Cat#24593; RRID: Addgene_24593
AAVretro-hSyn-Cre	Addgene	Cat#105553; RRID: Addgene_105553
AAVretro-CAG-tdTom	Addgene	Cat#59462; RRID: Addgene_59462
AAV8-hsyn-DIO-hM4Di-mCherry	Addgene	Cat#44362; RRID: Addgene_44362
AAV5/AAV8-hsyn-DIO-hM3Dq-mCherry	Addgene	Cat#44361; RRID: Addgene_44361
AAV9/AAV8-hsyn-DIO-mCherry	Addgene	Cat#50459; RRID: Addgene_50459
AAV1-AAV-syn-FLEX-jGCaMP8s-WPRE	Addgene	Cat#162377; RRID: Addgene_162377
pOTTC1032-AAVretro-EF1a-Nuc-flox(mCherry)-EGFP	Addgene	Cat#112677; RRID: Addgene_112677
AAVDJ-CBA-Cre-eGFP	Addgene	Cat#49056; RRID: Addgene_49056
AAV9-Syn-tTA-TRE-DIO-δLight	UNC Neurotools	N/A
AAV5-CAG-FLExloxP-TVA-mCherry	Addgene	Cat#48332; RRID: Addgene_48332
AAV8-CAG-FLExloxP-RABV-G	Addgene	Cat#48333; RRID: Addgene_48333
AAVretro-hSyn-Cre-P2A-dTomato	Addgene	Cat#107738; RRID: Addgene_107738
RABVdG-EnvA-H2B-GFP	*Gift From Lindsay Schwarz*	N/A
Chemicals, peptides, and recombinant proteins		
Clozapine-N-oxide (CNO)	Hello Bio	Cat#HB6149
Morphine Sulfate (CII)	Spectrum Chemicals	Cat#M1167
Naloxone Hydrochloride	Tocris	Cat#0599
4-Hydroxytamoxifen (4-OHT)	Tocris	Cat#3412
Complete Freund's Adjuvant (CFA)	Sigma	Cat#F5881
α-methyl-4,5-dimethoxy-2-nitrobenzene naloxone (PhNX)	McClain et al.[58]	N/A
Experimental models: Organisms/strains		
Mouse: C57Bl/6J	Jackson Labs	Strain#000664; RRID: IMSR_JAX:000664
Mouse: C57BL/6-*Oprm1*$^{tm2.1(EGFP/cre)Ics}$/KffJ (OPRM1-Cre)	Jackson Labs	Strain#038053; RRID: IMSR_JAX:038053
Mouse: B6J.129S6(FVB)-*Slc17a6*$^{tm2(cre)Lowl}$/MwarJ (vGlut2-Cre)	Jackson Labs	Strain#028863; RRID: IMSR_JAX:028863
Mouse: Fos$^{tm2.1(icre/ERT2)Luo}$/J (TRAP2)	Jackson Labs	Strain#030323; RRID: IMSR_JAX:030323
Software and algorithms		
Matlab 2021a	MathWorks	RRID: SCR_001622
Igor Pro 6	Wavemetrics	RRID: SCR_000325
pMAT	Bruno et al.[82]	N/A
Photoshop (Multiple Versions)	Adobe	RRID: SCR_014199
ImageJ (Multiple Versions)	NIH	RRID: SCR_003070
SMART v3.0.06	Panlab	RRID: SCR_002852
GraphPad Prism (Multiple Versions)	Graphpad	RRID: SCR_002798

(*Continued on next page*)

Please cite this article in press as: Livrizzi et al., Top-down control of the descending pain modulatory system drives multimodal placebo analgesia, Neuron (2026), https://doi.org/10.1016/j.neuron.2026.03.025

CellPress
OPEN ACCESS

Continued

REAGENT or RESOURCE	SOURCE	IDENTIFIER
BZ-X Analyzer Software	Keyence	RRID: SCR_023604
Illustrator	Adobe	RRID: SCR_010279
Bonsai	Lopes et al.[83]	RRID: SCR_021512

EXPERIMENTAL MODEL AND STUDY PARTICIPANT DETAILS

Animals

All procedures were approved by the UC San Diego, UC Irvine, or UPenn Institutional Animal Care and Use Committee and guidelines of the National Institute of Health. Mice were housed 1–5 per cage and maintained on a 12-hour reversed light/dark cycle in a temperature-controlled environment with *ad libitum* access to food and water. Experiments were performed under red lighting during the dark period using either C57Bl/6J mice (Jackson Laboratory, stock #000664, males, aged 8–60 weeks), *Oprm1-Cre* knock-in mice (Jackson Laboratory, stock #038053, aged 8-60 weeks), *vGlut2*-IRES-Cre knock-in mice (Jackson Laboratory, stock #028863, aged 8–60 weeks), or TRAP2 mice (Jackson Laboratory, stock #030323, aged 8-12 weeks).

METHOD DETAILS

Drugs

Clozapine-N-oxide (CNO) was purchased from Hello Bio, (HB6149). Morphine (mor) was purchased from Spectrum Chemicals (M1167). Saline solution was purchased from Teknova (S5819). Naloxone hydrochloride (NLX) was purchased from Tocris (0599). 4-hydroxytamoxifen (4-OHT) was purchased from Tocris (3412). Photoactivatable Naloxone (PhNX) was synthesized according to the published procedure[58] and purified to greater than 99.9% purity.

Viral constructs

The following viruses were obtained from Addgene: AAVretro-pgk-Cre (Addgene 24593, titer 1×10^{13} GC/ml), AAVretro-hSyn-Cre (Addgene 105553-AAVrg, titer $2.1x10^{13}$ GC/ml), AAVretro-CAG-tdTom (Addgene 59462, titer 1.2×10^{12} GC/ml), AAV8-hsyn-DIO-hM4Di-mCherry (Addgene 44362, titer $2.3x10^{12}$ GC/ml), AAV5 or AAV8-hsyn-DIO-hM3Dq-mCherry (Addgene 44361, titer $2.1x10^{12}$ GC/ml), AAV9 or AAV8-hsyn-DIO-mCherry (Addgene 50459, titer $3.5x10^{12}$ GC/ml), AAV1-AAV-syn-FLEX-jGCaMP8s-WPRE (162377, titer 2.3×10^{12} GC/ml), pOTTC1032-AAVretro-EF1a-Nuc-flox(mCherry)-EGFP (Addgene 112677, titer $2.5x10^{13}$ GC/ml). AAV-DJ-CBA-Cre-eGFP (Addgene 49056, titer 4.3×10^{12} GC/ml) was produced in house using plasmid obtained from Addgene and purified by ultracentrifugation with an iodixanol gradient. Titer was determined by qPCR. AAV9-Syn-tTA-TRE-DIO-δLight (titer 4.93×10^{12} GC/ml) was obtained from UNC Neurotools.

Surgery

Before surgery, mice were deeply anesthetized by induction at 5% isoflurane and maintained at 2% isoflurane (SomnoSuite, Kent Scientific). After mice were placed in a stereotaxic frame (David Kopf Instruments), a midline incision was made through the scalp following fur removal and site preparation by alternating povidone-iodine and 70% isopropyl alcohol. 150-250 nl of virus was injected at a rate of 100 nl/min. The following coordinates were used for viral injection and optical fiber implantation, with DV indicating the distance ventral to skull. vlPAG: (angle ±10°) AP−4.60 mm, ML ±0.32 mm, DV 2.72 mm; RVM: (bilateral, angle -10°) AP -7.00 mm, ML +0.26 and -0.67 mm, DV +6.30 and +6.26 mm; ACC: AP 1.20 mm, ML ±0.30 mm, DV 2.52 mm; mPFC: AP 1.98 mm, ML ±0.30 mm, DV 2.20 mm; AI: AP 2.0, ML -2.50 mm and +2.20 mm, DV 3.20 mm. Following all surgeries, mice were administered ketoprofen (5 mg/kg, i.p., MWI Veterinary Supply) before the end of surgery and 24 hours later and monitored for recovery for 5 days. Mice were given at least one week to recover from cannula or optical implant surgeries before behavior or fiber photometry experiments.

Chemogenetic manipulation

In all experiments, experimenters were blind to the AAV with which experimental animals were transduced (DREADD or mCherry control). Mice underwent behavioral testing 6 weeks after viral injection. The dose of CNO (3 mg/kg) was chosen based on published studies and was confirmed to induce robust cFOS expression in hM3Dq-labeled neurons in our hands (data not shown). In morphine analgesia experiments, CNO was injected *i.p.* 60 min before beginning behavioral test followed by *i.p.* injection of morphine (5 mg/kg, 10 mg/kg and 20 mg/kg) 30 min later.

Pain behavior assessment

Prior to all behavioral testing mice were acclimated to the testing room for at least one hour. Repeated testing of individual mice was conducted at the same time each day by the same experimenter. In this study, all experimenters conducting behavioral tests were

Please cite this article in press as: Livrizzi et al., Top-down control of the descending pain modulatory system drives multimodal placebo analgesia, Neuron (2026), https://doi.org/10.1016/j.neuron.2026.03.025

female. In all instances, the experimenter was blinded to drug and/or virus identity on test day. In general, experiments were conducted with two separate cohorts containing control and experimental subjects in roughly equal numbers (~8 mice per cohort). This counterbalancing was conducted to ensure that potential loss or reduction in the placebo effect is due to the experimental manipulation. Pooled data from both cohorts are reported.

Hot Plate Test

Mice were initially placed on a room temperature hot plate in a chamber (clear plexiglass cylinder or one harboring contextual cues) adjacent to the testing hot plate (ThermoFisher Scientific, HP88857100), which was set to 52 °C. After at least 5 minutes of acclimation (longer for conditioning, as described), mice were transferred with the chamber to the 52 °C hot plate, and the latency to first hind paw withdrawal was measured. Mice were immediately removed from the hot plate after exhibiting the first hind paw withdrawal. A withdrawal was counted as the first instance of a mouse rapidly lifting, shaking, licking/biting their paw, or jumping. Withdrawal latencies were measured three times, with a five-minute break between trials. During the break mice were kept alone in an empty cage and placed directly on the 52 °C hot plate for the 2nd and 3rd trials of each session. Data are reported as the average of the three trials unless otherwise noted. The cutoff time on the hot plate was 60 seconds to prevent tissue damage.

The inescapable hot plate test was conducted as described above but mice were left on the hot plate for 60 sec. The latency to first jump and the total number of jumps during the 60 sec period were recorded across three trials (5 min intervals).

Von Frey Test

Mice were placed on an elevated wire mesh platform and allowed to acclimate for 15 minutes prior to testing using the up-down method,[84] von Frey filaments of varying stiffness were applied to the plantar surface of each hind paw separately until a withdrawal response could be recorded, and a 50% withdrawal threshold could be calculated. Filaments were applied in 2-5-minute intervals before returning to the first paw to avoid sensitization.

Pinprick Test

Mice were placed on an elevated wire mesh platform and allowed to acclimate for 15 minutes prior to testing. A fine insect pin (size 000, Thermo Fisher Scientific, NC9295307) was lightly applied to the plantar surface of each hind paw five times at 2–5-minute intervals each for a total of 10 applications. Care was taken to ensure the pin did not puncture the skin. Values displayed represent the number of trials out of the 10 wherein the mouse displayed nocifensive behavior (withdrawal, shaking, licking, or biting) in response to the pin.

Hot Plate Placebo Conditioning

Other than in Figures 1N–1P, placebo experiments were conducted in male mice. Other than in Figure 5 (pain modality transfer), a parallel experimental design was used, with control mice being run in parallel with an experimental manipulation group.

In placebo protocol 1, mice were conditioned for 4 consecutive days using alternating injections saline (0.9%, 4 μL/gram of body weight, *i.p.*) on days 1 and 3 or morphine (10 mg/kg, i.p.) on days 2 and 4. Following administration, mice were immediately placed in a cylindrical conditioning chamber (4.5'' diameter, 8'' height) endowed with distinct contextual cues composed of a combination of visual cues (diagonal stripes or dots) and olfactory cues (limonene (citrus) or isoamyl acetate (banana), 1% odorant in mineral oil). Although *n*-pentyl acetate, another banana-like odorant, has been found to produce stress-induced analgesia in male mice,[85] isoamyl acetate did not alter hot plate paw withdrawals. Within cohorts, odorants were counterbalanced with the visual cues and drug treatments. For simplicity, the schematics in the figures only show one contextual cue combination for each drug condition. Odorants were presented by suspending a cotton swab saturated with 120 μL of the odorant/mineral oil mixture, such that a standing mouse could not reach the tip. After 30 min on the room-temperature hot plate in the conditioning chamber, mice were transferred to the 52 °C hot plate for the hot plate test (3 trials). On day 5, the mice were administered saline and then placed in the conditioning chamber previously paired with morphine, prior to the hot plate test.

Placebo protocol 2 omits the interleaved saline treatment and doubles the number of morphine exposures each day. On pre-test day, mice were administered saline (4 μL/gram of body weight, *i.p.*) and acclimated for 30 min on a room temperature hot plate in a chamber (clear plexiglass cylinder) that lacked contextual cues prior to the hot plate test. On conditioning days 1 and 2, mice were injected with morphine (10 mg/kg, i.p.) once in the morning (AM) prior to placement in the conditioning chamber and hot plate test, and again 3.5 hours later (PM) followed by the same conditioning and test sequence. Between AM and PM sessions, mice were singly housed in a cage with *ad libitum* water. Mice were returned to their home cages following the conclusion of the PM session. On day 3 (test day), the mice were administered either saline (4 μL/gram of body weight, *i.p.*), CNO (3 mg/kg, i.p.), naloxone (3 mg/kg, i.p.), or PhNX (30 mg/kg, i.p.) and then placed in the conditioning chamber associated with morphine for 30 min followed by the hot plate test.

To calculate the percentage of morphine effect in the placebo experiments, we applied the following formula to the data acquired from individual mice:

$$\%\ \text{morphine effect} = \frac{\textit{placebo test latency} - \textit{saline day 1 latency}}{\textit{final morphine dose latency} - \textit{saline day 1 latency}} * 100$$

Please cite this article in press as: Livrizzi et al., Top-down control of the descending pain modulatory system drives multimodal placebo analgesia, Neuron (2026), https://doi.org/10.1016/j.neuron.2026.03.025

CellPress
OPEN ACCESS

Mice were considered to be placebo responders if they exhibited withdrawal latencies on the placebo test ≥3 standard deviations greater than the saline day 1 (pre-test) mean latency of the pooled cohorts.

Unpaired control conditioning procedure

Mice were conditioned using placebo protocol 1 to associate morphine with the context but not pain relief by first being tested on the hot plate without receiving an injection. Within minutes of completing the hot plate test, mice were administered morphine (10 mg/kg, i.p.) and placed on a room temperature hot plate, within a conditioning chamber. After 30 minutes they were returned to their home cages.

Placebo-related locomotion

Locomotion was measured for one cohort of mice within the conditioning chambers during a placebo conditioning sequence with placebo protocol 2 using a video camera mounted above the open-top cylinders. Total distance travelled in the 10-30 min period following saline or morphine injection was determined from the videos using PanLabs SMART software.

Extinction and reconditioning

Mice were conditioned using placebo protocol 2 but tested for placebo once a day (3 trials/day) for 5 consecutive days after conditioning. On the 6th day post-conditioning (no injection), mice were not injected with saline or placed in a conditioning chamber, but instead tested on the hot plate within a clear cylinder directly from their home cage. On the 7th day post-conditioning, mice were re-conditioned with morphine (10 mg/kg, i.p.) twice (AM, PM) as in protocol 2, and tested for reconditioned placebo (rc placebo) on the 8th day post-conditioning.

Opioid-induced hyperalgesia (OIH)

One day prior to placebo conditioning on the hot plate, following administration of saline to control for injection stress, mice were assessed using the von Frey test. The von Frey test was conducted in a different room than placebo conditioning in the absence of the contextual cues used for conditioning. After conditioning with morphine on the hot plate, instead of conducting a placebo test, mice were taken back to the room used for the von Frey baseline test, injected with saline, and assessed using the von Frey test. Male and female mice were tested on the same day.

TRAP conditioning

A modified version of conditioning protocol 2 was used for the TRAP experiments. Protocol efficacy for producing placebo analgesia was established in the following manner (data shown in Figure S2B). Separate groups of C57BL/6J mice were conditioned for 4 consecutive days, via injection with either vehicle solution or morphine (10 mg/kg, s.c.) dissolved in vehicle solution. The vehicle solution was comprised of 200 proof ethanol (10% final volume), kolliphor oil (20% final volume), and sterile 1x phosphate buffered saline (PBS, 70% final volume). The vehicle solution was used to acclimate mice for the targeted recombination in active populations (TRAP) procedure, described below. Immediately following injections, mice were placed in individual room-temperature cylindrical plastic containers (3'' diameter, 6'' height) with mango-scented odorant cue dissolved in mineral oil and applied to a q-tip outside of the container. Mice remained in the containers for 1 hour prior to transfer to a pre-heated hotplate set to 52.5°C for a maximum of 30 seconds. The animal's latency to respond by hindpaw withdrawal was recorded. For the test on Day 5, all mice received the vehicle solution followed by placement in the conditioning chambers for 1 hour and then transfer to the 52.5°C hotplate.

Placebo context TRAP

At least two weeks after intracranial AAV injection, separate groups of TRAP2 mice were conditioned for 4 consecutive days, via injection with either vehicle solution or morphine (10 mg/kg, s.c.) dissolved in vehicle solution, as described above. Immediately following injections, mice were placed in individual room-temperature containers (6.5'' width, 6.5'' depth, 13'' height) with horizontal black and white stripe visual cues and banana-scented odorant cue dissolved in mineral oil and applied to a q-tip outside of the container. The container floors consisted of brushed aluminum, similar to the texture of the hotplate. Mice remained in the containers for 1 hour prior to transfer to a pre-heated hotplate set to 52.5°C for a maximum of 45 seconds. TRAP induction occurred on Day 5, with all mice receiving tamoxifen (4-OHT; 20-40 mg/kg, *s.c.*) dissolved in vehicle solution just prior to placement in the conditioning containers for 2 hours followed by return to the home cage.

TRAP reactivation

30 days after the TRAP procedure was completed, mice underwent reactivation testing. Mice were tested using an inescapable hotplate test 40 minutes after injection of saline or CNO (3 mg/kg, i.p.). Here, the hotplate was pre-heated to 50°C, with a clear plastic container and no visual or odorant cues. The time to withdrawal one of the hind paws was recorded.

Pinprick Placebo Conditioning

Mice were conditioned as in placebo protocol 2 using the pinprick rather than the hot plate test.

Pain Modality Transfer Experiments

A crossover design was used such that all mice were tested on placebo day after administration of either saline or naloxone. In the first leg, half of the mice were administered naloxone (3 mg/kg, i.p.) and the other half were administered 0.9% sterile saline (4 μL/gram of body weight, *i.p.*). To complete the crossover, mice were reconditioned and tested 3 weeks later in the same manner, but mice originally administered saline were given naloxone, and vice versa. The placebo test day data are pooled in the main figures but shown chronologically in Figure S5. Detailed schematics for the transfer experiments are also shown in Figure S5.

Please cite this article in press as: Livrizzi et al., Top-down control of the descending pain modulatory system drives multimodal placebo analgesia, Neuron (2026), https://doi.org/10.1016/j.neuron.2026.03.025

On Day 1, 24 hours prior to initiating conditioning, mice were tested for baseline responses to both the hot plate and pinprick tests. Mice were counterbalanced such that half were tested on the hot plate in the AM and the pinprick assay in the PM, or vice versa. Prior to both tests, mice received 0.9% sterile saline (4 μL/gram of body weight, *i.p.*) and were allowed to acclimate in a clear cylinder for 30 minutes.

Relay pain modality transfer procedure

The same procedure was used for the hot plate → pinprick and pinprick → hot plate relay experiments. After acquiring baseline responses to both tests on Day 1, mice were conditioned using either the hot plate or the pinprick test with morphine (10 mg/kg, i.p.) according to protocol 2. On Day 4 (test day), mice were given either saline or naloxone. After completing the placebo test with the source pain modality, mice were immediately transferred along with their morphine-paired conditioning chambers to the other pain modality test, which began within 30 seconds of completing the first placebo test.

Substitution pain modality transfer procedure

The procedure used was identical to the relay experiment except on test day. After administration of either saline or naloxone, mice were placed in their morphine-paired conditioning chamber on the source modality surface (a room temperature hot plate or the elevated wire mesh platform). After 30 min and they were moved along with their conditioning chamber to the recipient test modality (wire mesh platform or 52 °C hot plate, respectively) for immediate testing.

Hot plate → CFA → von Frey pain prevention procedure

Pain naïve mice were first conditioned on the hot plate with morphine (10 mg/kg, i.p.) using protocol 2. Following the initial hot plate placebo test day (day 4), mice were reconditioned with morphine on day 5. On the morning of day 6, undiluted Complete Freund's Adjuvant (CFA, 5 μL) was injected into the plantar region of the left hind paw.[86] In the afternoon 3.5 hours later, mice were administered saline in the morphine/hot plate-context but tested with the von Frey assay using the substitution pain modality transfer procedure. The hot plate → von Frey substitution placebo test was repeated on days 7, 8, 9, and 10. On day 10, all mice received naloxone (3 mg/kg, i.p.) in lieu of saline.

The unpaired conditioning procedure, adapted to the repeated morphine treatment sequence in placebo protocol 2, was used as a negative control. Pain naïve mice were conditioned to associate morphine with the context but not pain relief by first being tested on the hot plate without receiving an injection. The subsequent hot plate placebo tests and hot plate → von Frey substitution tests were conducted as described above.

Fiber photometry

For fiber photometry recordings in vlPAG from vlPAG→RVM neurons, C57Bl/6J mice were injected bilaterally in the RVM with AAVretro-hSyn-Cre (150 nl per injection) and unilaterally in the right vlPAG with a 1:1 mixture of AAV1-syn-FLEX-jGCaMP8s + AAVDJ-hsyn-DIO-mCherry (150 nl) and implanted unilaterally in the right vlPAG with a 200 μm diameter optical fiber. For recordings of δLight in vlPAG, *Oprm1-Cre* mice were unilaterally injected in the right vlPAG with AAV9-Syn-tTA-TRE-DIO-δLight (150 nl) and implanted in the vlPAG with a 200 μm diameter optical fiber. Recordings were made using a Neurophotometrics FP3001 fiber photometry system at a sampling rate of 33 Hz, data acquisition was conducted in Bonsai. A 470 nm LED was used to record GCaMP activity with a 560 nm LED for the mCherry control channel. For δLight recordings, a 470 nm LED was used to record δLight activity and 415 nm LED (isosbestic point) was used as control. Data analysis of fluorescence recordings was conducted using the pMAT open source photometry analysis package[82] in MATLAB 2021a (Mathworks), which allows for the scaling of the red control channel to correct for movement and bleaching, and subsequently calculates peri-event time histograms of ΔF/F and z-score values. Other calculations, such as baseline correction, downsampling, and area under the curve analysis, were completed in Igor Pro (Wavemetrics). Fluorescence traces are presented in the figures as the mean ± SEM of single traces (hot plate trial 1) from all mice.

In vivo drug uncaging

Ultraviolet light was delivered to the mouse brain through optical fibers (200 μm diameter, high-OH, 1.25 mm ceramic ferrule) implanted bilaterally over the vlPAG. Light from a 375 nm laser (Oxxius, LBX-375-400-HPE-PPA) was launched into two 200 μm diameter, high-OH fiber optic cables (Thorlabs) using a custom-built light path that included a 50/50 UV beamsplitter to direct the light into the two fiber optic cables. Light power was calibrated immediately prior to use to deliver 30 mW from the cable tip. Transmission through optical fibers prior to implantation was ∼75% such that estimated power delivery to the brain was ∼22.5 mW. Light pulses (10 x 200 ms, 1 Hz) were generated in response to experimenter-controlled switch by an Arduino UNO.

For PhNX uncaging during morphine analgesia, after being bilaterally connected to the fiber optic cables, mice were injected with PhNX (30 mg/kg, i.p), returned to their home cage for 10 min and then assessed for baseline thermal nociception on the hot plate test. For 'early' uncaging experiments, PhNX was photoactivated 1 min before injection of morphine (5 mg/kg, i.p). Subsequently, thermal nociception was assessed on the hot plate every 10 min for a total of 60 min. For 'late' uncaging experiments, PhNX was photoactivated 37 minutes after morphine injection. For the no-light control experiments, PhNX was never photoactivated although the fiber optic cables were connected. For this experiment, hot plate measurements were only taken once per time point.

For experiments involving uncaging during placebo analgesia, baseline thresholds were acquired, and mice were conditioned while bilaterally connected to the fiber optic cables (no light was applied). On placebo test day mice were injected with either saline

or PhNX (30 mg/kg, i.p) prior to placement in the morphine-conditioned context. Light flashes were triggered 3 minutes before placing mice on the hot plate (3 trials, 5 min interval, light administered on each trial).

RABV monosynaptic tracing

To map monosynaptic inputs to ventrolateral periaqueductal gray (vlPAG) neurons projecting to the rostroventral medulla (RVM), in C57BL/6J mice we injected 500 nL of a 1:1 helper AAV mixture—AAV5-CAG-FLExloxP-TVA-mCherry (3.1 x 10^{12} gc/mL; Addgene #48332) and AAV8-CAG-FLExloxP-RABV-G (2 x 10^{12} gc/mL; Addgene #48333)—was stereotaxically injected into the vlPAG (AP −4.78 mm, ML −0.70 mm, DV −2.75 mm). To restrict starter cells to the vlPAG population projecting to the RVM, 500 nL of AAVretro-hSyn-Cre-P2A-dTomato (7×10^{12} gc/mL; Addgene #107738) was delivered bilaterally to the RVM (AP −7.20 mm, ML ±0.33 mm, DV −5.75 mm). Two weeks after AAV injection, 500 nL of glycoprotein deleted, EnvA-pseudotyped, GFP-expressing RABV encoding nuclear GFP (RABVΔG-EnvA-H2B-GFP; 6.2 x 10^{8} cfu/mL) was injected into the same vlPAG coordinates to initiate retrograde monosynaptic tracing. Five days after RABV injection, animals were deeply anesthetized and transcardially perfused first with phosphate-buffered saline (PBS) to clear blood, followed by 4% formaldehyde (PFA) for fixation. Brains were extracted, post-fixed overnight in PFA at 4 °C, and coronally sectioned at 60 μm. Every section was mounted sequentially in anterior-to-posterior order to maintain anatomical continuity. To ensure the integrity of anatomical targeting and data interpretation, post-hoc histological validation of viral injection sites was performed for every experimental animal. Only data from animals with confirmed and accurately localized viral expression were included in quantitative analyses.

RABV Mapping

Fluorescently labeled brain sections were imaged using an Olympus IX83 inverted epifluorescence microscope (Olympus, Japan) equipped with an Olympus CBH IX3 control unit and a motorized Marzhauser Wetzlar Tango stage. Illumination was provided by an X-Cite Xylis LED light source. Imaging was performed using UPlanSApo 4×/0.16 NA and UPlanSApo 10×/0.40 NA objectives with a 0.55 NA optical path configuration. Images were acquired using CellSens Dimension software (v3.2) with an Olympus XM10 digital camera coupled via a U-TV1XC adapter. Appropriate fluorescence filter sets were used to visualize GFP-expressing RABV-labeled and mCherry-expressing TVA-labeled cells. Exposure time, gain, and illumination intensity were held constant across samples within each experimental group. GFP-expressing input cells were manually counted in Photoshop using a one-in-three sampling scheme: for every three consecutive sections, only the first section was quantified to avoid repeated counts of the same neurons across neighboring sections. To restrict quantification to bona-fide monosynaptic inputs, a starter-zone exclusion was enforced: all GFP-positive inputs within a 1-mm radius of the vlPAG RABV injection site were excluded, mitigating local labeling attributable to high EnvA–TVA affinity. For each region, the number of GFP-positive inputs was divided by the total number of GFP-positive inputs counted across the entire brain to yield the proportion of inputs expressed as a percentage (% of total RABV-labeled inputs). These values were used to generate regional input distribution profiles. All statistical analyses were performed using GraphPad Prism. Data are presented as mean ± SEM.

Histology

Mice were transcardially perfused with 25 mL ice-cold PBS followed by 25 mL ice-cold 4% paraformaldehyde (PFA). Brains were harvested and post-fixed in 4% PFA overnight at 4°C, then transferred to a 30% sucrose solution and stored at 4°C until sectioning. Brains were sliced into 40 μm sections using a freezing microtome (Microm 450, Thermo Scientific) and stored in PBS at 4°C until processing for immunohistochemistry. Non-immunostained sections were immediately mounted on coverslips in DAPI-containing mounting medium (Vector Laboratories, #H1200).

For Figures S3F–S3I, immunohistochemical staining for cFOS was performed as follows: free-floating brain slices were blocked in 5% NDS (normal donkey serum) in PBS supplemented with 0.3% TritonX (PBST) for 2 hrs at RT, then transferred to a solution containing guinea pig anti-cFOS primary antibody (1:1,000, Synaptic Systems 226 308) in 1% NDS in PBST 0.3%, and shaken gently for 48 hrs at 4°C. Sections were then washed 3x for 10 min in PBS at RT and transferred to a solution containing Alexa 488-conjugated goat anti-guinea pig secondary antibody (1:1,000, Abcam 150185) and 1% NDS in 0.1% PBST, then shaken gently for 2 hrs at RT. Sections were washed 3x for 10 min in PBS at RT and mounted with DAPI-containing mounting medium. For both stained and non-stained tissue, sections were imaged on a Keyence microscope (BZ-X710) at ×2, ×10, or ×20 magnification. Cell counts for cFOS positive neurons were performed in ImageJ.

TRAP mouse histology

TRAP mice were anesthetized using FatalPlus (Vortech) and transcardially perfused with 1x PBS, followed by 10% neutral buffered formalin solution (NBF, Sigma, HT501128). Brains were quickly removed and post-fixed in 10% NBF for 24 hours at 4 °C, and then cryo-protected in a 30% sucrose solution made in 1x PBS until sinking to the bottom of the storage tube (∼48 h). Brains were then frozen in Tissue Tek O.C.T. compound (Thermo Scientific), coronally sectioned on a cryostat (CM3050S, Leica Biosystems) at 30 μm or 50 μm and the sections were stored in 1x PBS. Floating sections were permeabilized in a solution of 0.3% PBST for 30 min at room temperature and then blocked in a solution of 0.3% PBS-T and 5% NDS for 2 hours before being incubated with primary antibodies (1°Abs included: chicken anti-GFP [1:1000, Abcam, ab13970], rabbit anti-DsRed [1:1000, Takara Bio, 632496], prepared in a 0.3% PBST, 5% NDS solution for ∼16-20 h at room temperature. Following washing three times for 10 min each in PBST, secondary antibodies (2°Abs included: Alexa-Fluor 488 donkey anti-chicken [1:500, Jackson Immuno, 703-545-155], Alexa-Fluor 594 donkey

Please cite this article in press as: Livrizzi et al., Top-down control of the descending pain modulatory system drives multimodal placebo analgesia, Neuron (2026), https://doi.org/10.1016/j.neuron.2026.03.025

anti-rabbit [1:500, Thermo Scientific, A21207], prepared in a PBST, 5% NDS solution were applied for ~2h at room temperature, after which the sections were washed again three times for 5 mins each in 1x PBS, then again three times for 10 min in 1x PBS, and then counterstained in a solution of 1x PBS containing DAPI (1:5,000, Sigma, D9542). Fully stained sections were mounted onto Superfrost Plus microscope slides (Fisher Scientific) and allowed to dry and adhere to the slides before being coated with Fluoromount-G Mounting Medium (Invitrogen, 00-4958-02) and cover slipped.

All tissue was imaged on a Keyence BZ-X all-in-one fluorescent microscope at 48-bit resolution using the following objectives: PlanApo- λ x4 and PlanApo- λ x20. All image processing prior to quantification was performed with the Keyence BZ-X analyzer software (version 1.4.0.1). Quantification of neurons expressing fluorophores was performed via manual counting of TIFF images in Photoshop (Adobe, 2021) using the Counter function. Counts were made using 20X magnified z-stack images.

Statistics

Throughout the manuscript, data are represented as the mean±SEM. Data were analyzed in GraphPad Prism. All datasets were evaluated for normality using the D'Agostino and Pearson test and the Shapiro-Wilk test. Normally-distributed datasets were analyzed using parametric statistics and non-normally-distributed data sets were analyzed using non-parametric statistics, taking into account repeated measures from individual subjects when appropriate. P values are presented in the figures. The number of experimental replicates and the statistical test used are presented in each figure legend. In some cases, when cohorts were split into multiple conditions (e.g. saline vs. naloxone), instead of a two-way ANOVA, the equivalent Mixed-effects model was used to allow for missing data. Not all statistically significant comparisons are indicated in the figures. Raw data, summary data, and statistical test details (including F and t values, and degrees of freedom) for each graph are available in the Source Data spreadsheet.

Neuron, Volume *114*

Supplemental information

Top-down control of the descending pain modulatory system drives multimodal placebo analgesia

Giulia Livrizzi, Janie Chang-Weinberg, Desiree A. Johnson, Susan T. Lubejko, Jingzhu Liao, Blake A. Kimmey, Chunyang Dong, Yuan Li, Kevin T. Beier, Gregory Corder, Lin Tian, and Matthew R. Banghart

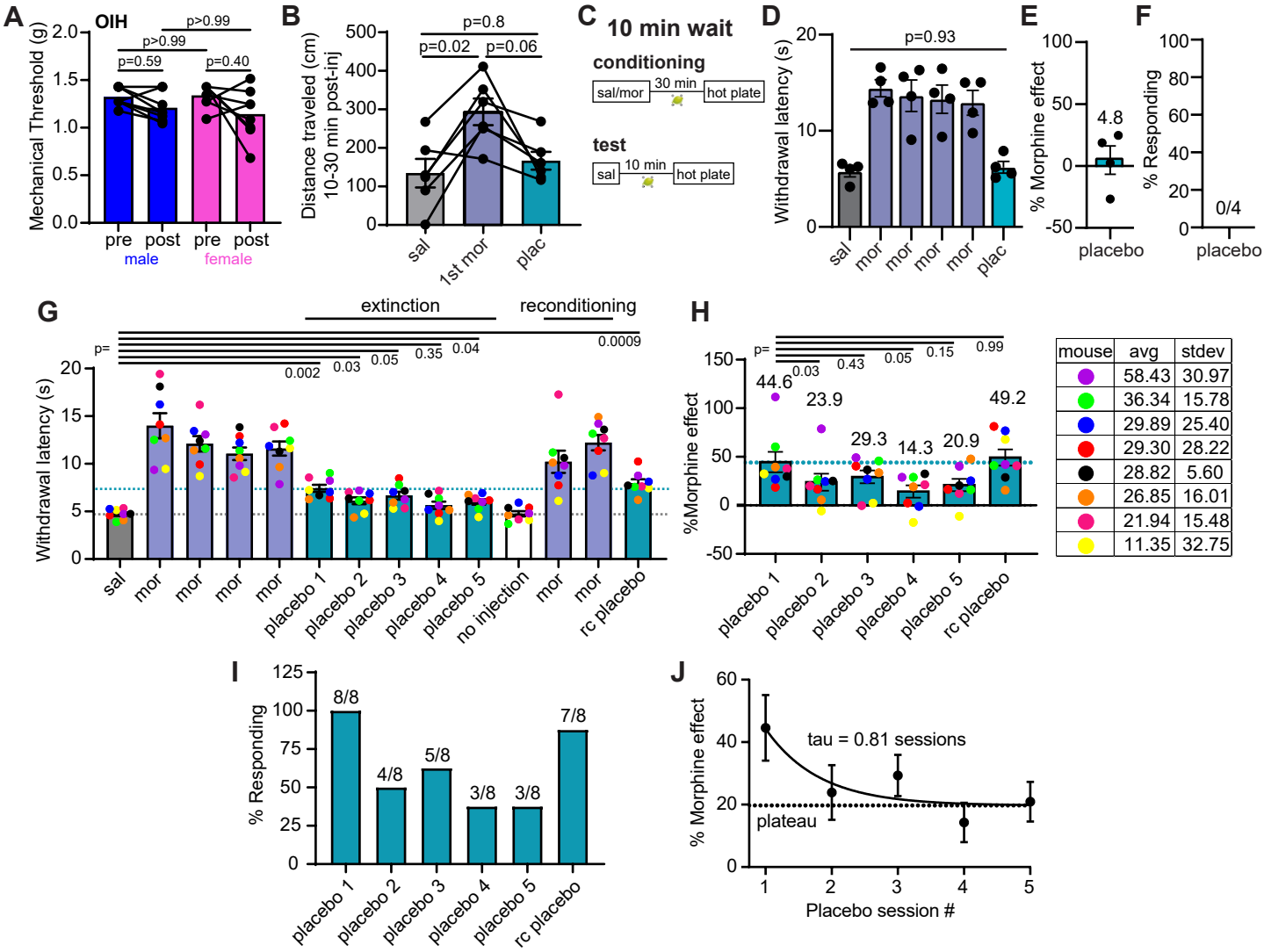
A
OIH
p>0.99
p>0.99
p=0.59
p=0.40
Mechanical Threshold (g)
pre post pre post
male female
B
p=0.8
p=0.02 p=0.06
Distance traveled (cm) 10-30 min post-inj
sal 1st mor plac
C
10 min wait
conditioning
sal/mor 30 min hot plate
test
sal 10 min hot plate
D
p=0.93
Withdrawal latency (s)
sal mor mor mor mor plac
E
% Morphine effect
4.8
placebo
F
% Responding
0/4
placebo
G
extinction
reconditioning
p=
0.002 0.03 0.05 0.35 0.04 0.0009
Withdrawal latency (s)
sal mor mor mor mor placebo 1 placebo 2 placebo 3 placebo 4 placebo 5 no injection mor mor rc placebo
H
p=
0.03 0.43 0.05 0.15 0.99
%Morphine effect
44.6 23.9 29.3 14.3 20.9 49.2
placebo 1 placebo 2 placebo 3 placebo 4 placebo 5 rc placebo
mouse avg stdev
58.43 30.97
36.34 15.78
29.89 25.40
29.30 28.22
28.82 5.60
26.85 16.01
21.94 15.48
11.35 32.75
I
% Responding
8/8 4/8 5/8 3/8 3/8 7/8
placebo 1 placebo 2 placebo 3 placebo 4 placebo 5 rc placebo
J
% Morphine effect
tau = 0.81 sessions
plateau
Placebo session #

Figure S1: Further characterization of [morphine + noxious stimulus]-conditioned placebo analgesia, Related to Figure 1.

(**A**) Assessment of opioid-induced hyperalgesia (OIH) in response to Protocol 2 using the von Frey assay before and after conditioning (males: n=8, females: n=8, Friedman test with Dunn's multiple comparison post-hoc, p=0.15). (**B**) Distance travelled within the holding chamber (prior to the hot plate test) during the 10-30 min period after injection of saline, morphine (1st exposure), or saline on placebo test day, (n=10, RM on-way ANOVA with Tukey's post-hoc, F (1.83,9.12)=7.377, p=0.014). (**C**) Schematic describing the 30 vs. 10 minute wait period on conditioning and test days, respectively. (**D**) Hot plate paw withdrawal latencies before, during, and after conditioning for the protocol described in (**C**) (n=4, RM one-way ANOVA with Dunnett's post-hoc, F(1.60,4.80)=27.60, p=0.0027). (**E**) Placebo effect quantified as % of the response to the previous dose of morphine for the data shown in (**D**). (**F**) Placebo response quantified as the % of subjects exhibiting antinociception for the data shown in (**D**). (**G**) Hot plate paw withdrawal latencies before and after conditioning, rc = reconditioned (n=8, RM one-way ANOVA with Dunnett's post-hoc, F(3.25,22.71)=26.52, p<0.0001). Grey dotted line indicates average withdrawal latency for saline baseline (4.72 seconds), teal dotted line indicates average withdrawal latency for placebo 1 (7.425 seconds). (**H**) Same as (**E**), but for the data shown in (**G**); the average % morphine effect is indicated over each placebo day (RM one-way ANOVA with Dunnett's post-hoc, F(2.50,17.52)=3.89, p=0.032). Teal dotted line indicates average % morphine effect of placebo 1 (44.6%). The table summarizes the average placebo effect for each mouse over all testing sessions. (**I**) Same as (**F**), but for the data shown in (**G**). (**J**) Placebo effect extinction as a function of session number. Data were fit to a monoexponential function.

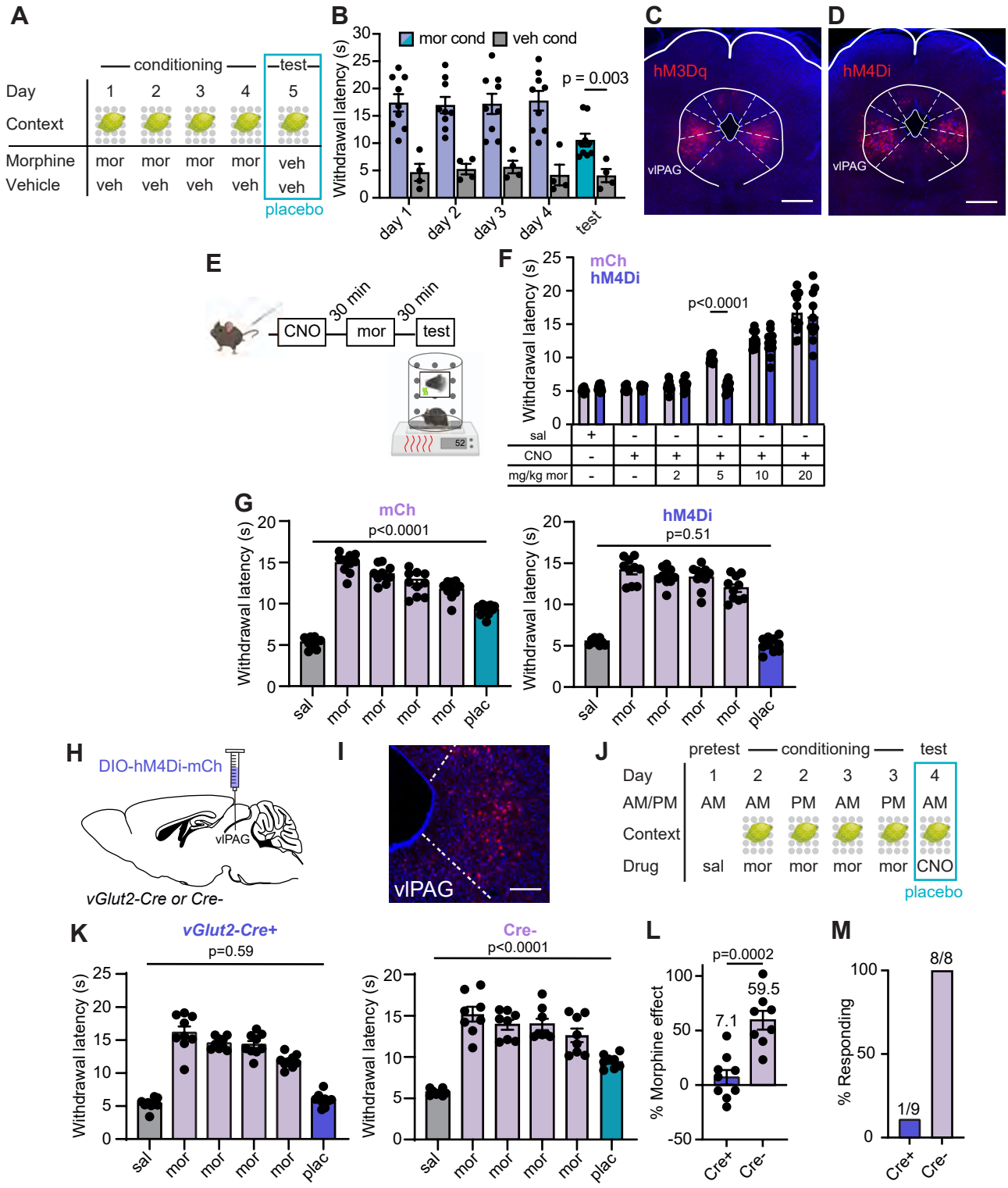
A
conditioning
test
Day
1 2 3 4 5
Context
Morphine
mor mor mor mor veh
Vehicle
veh veh veh veh veh
placebo
B
mor cond
veh cond
Withdrawal latency (s)
p = 0.003
day 1
day 2
day 3
day 4
test
C
hM3Dq
vlPAG
D
hM4Di
vlPAG
E
CNO
30 min
mor
30 min
test
F
mCh
hM4Di
p<0.0001
Withdrawal latency (s)
sal + - - - - -
CNO - + + + + +
mg/kg mor - - 2 5 10 20
G
mCh
p<0.0001
hM4Di
p=0.51
Withdrawal latency (s)
sal mor mor mor mor plac
H
DIO-hM4Di-mCh
vlPAG
vGlut2-Cre or Cre-
I
vlPAG
J
pretest
conditioning
test
Day 1 2 2 3 3 4
AM/PM AM AM PM AM PM AM
Context
Drug sal mor mor mor mor CNO
placebo
K
vGlut2-Cre+
p=0.59
Cre-
p<0.0001
Withdrawal latency (s)
sal mor mor mor mor plac
L
p=0.0002
% Morphine effect
7.1
59.5
Cre+ Cre-
M
% Responding
1/9
8/8
Cre+ Cre-

Figure S2: Chemogenetic silencing of vlPAG→RVM and vlPAG$^{vGlut2\text{-}Cre}$ neurons during placebo trials, Related to Figure 2.

(**A**) Schematic of the placebo protocol used for the TRAP experiments shown in **Figure 2A-F**. (**B**) Hot plate paw withdrawal latencies during and after conditioning (morphine conditioned: n=9, vehicle conditioned: n=4, Mann-Whitney, p=0.0028). (**C**) Example of hM3Dq-mCh expression in the vlPAG upon transduction with AAVretro-Cre in the RVM of a wildtype mouse. Scale bar = 500 μm (**D**) Same as in (**C**), but with hM4Di-mCh. Scale bar = 500 μm. (**E**) Schematic of the timeline for sequential CNO and morphine co-administration to match their onset kinetics for nociception analysis on the hot plate assay in **Figure 2L**. (**F**) Hot plate paw withdrawal latencies in response to saline or morphine (0, 2, 5, 10, 20 mg/kg) administration upon chemogenetic inactivation of vlPAG→RVM neurons with hM4Di vs. mCherry control (mCh: n=10, hM4Di: n=10, Two-way ANOVA with Tukey's post-hoc, drug x virus interaction $F(5,108)=5.49$, $p=0.0002$). (**G**) Hot plate paw withdrawal latencies before, during, and after conditioning upon chemogenetic silencing of vlPAG→RVM neurons on placebo test day for the data shown in **Figure 2M-O** (mCh: n=10, RM one-way ANOVA with Dunnett's post-hoc, $F(3.31,29.76)=122.8$, $p<0.0001$; hM4Di: n=10, RM one-way ANOVA with Dunnett's post-hoc, $F(3.01,27.07)=133.4$, $p<0.0001$). (**H**) Illustration of viral transduction of vlPAG$^{vGlut2\text{-}Cre}$ neurons with hM4Di. Cre-negative littermates were used as a negative control. (**I**) Example of hM4Di-mCh expression in the vlPAG of a *vGlut2-Cre* mouse. Scale bar = 250 μm. (**J**) Schematic of Protocol 2 indicating chemogenetic silencing with CNO administration on placebo test day. (**K**) Hot plate paw withdrawal latencies before, during, and after conditioning upon chemogenetic silencing of vlPAG$^{vGlut2\text{-}Cre}$ neurons on placebo test day (Cre-: n=8, RM one-way ANOVA with Dunnett's post-hoc,

F(2.79,19.54)=46.28, p<0.0001; Cre+: n=9, RM one-way ANOVA with Dunnett's post-hoc, F(2.12,16.97)=86.61, p<0.0001). (**L**) Placebo effect quantified as % of the response to the previous dose of morphine upon chemogenetic silencing of vlPAG$^{vGlut2\text{-}Cre}$ neurons for the data shown in (**K**) (Cre+: n=9, Cre-: n=8, unpaired t-test). (**M**) Placebo response in (**K**) quantified as the % of subjects exhibiting antinociception.

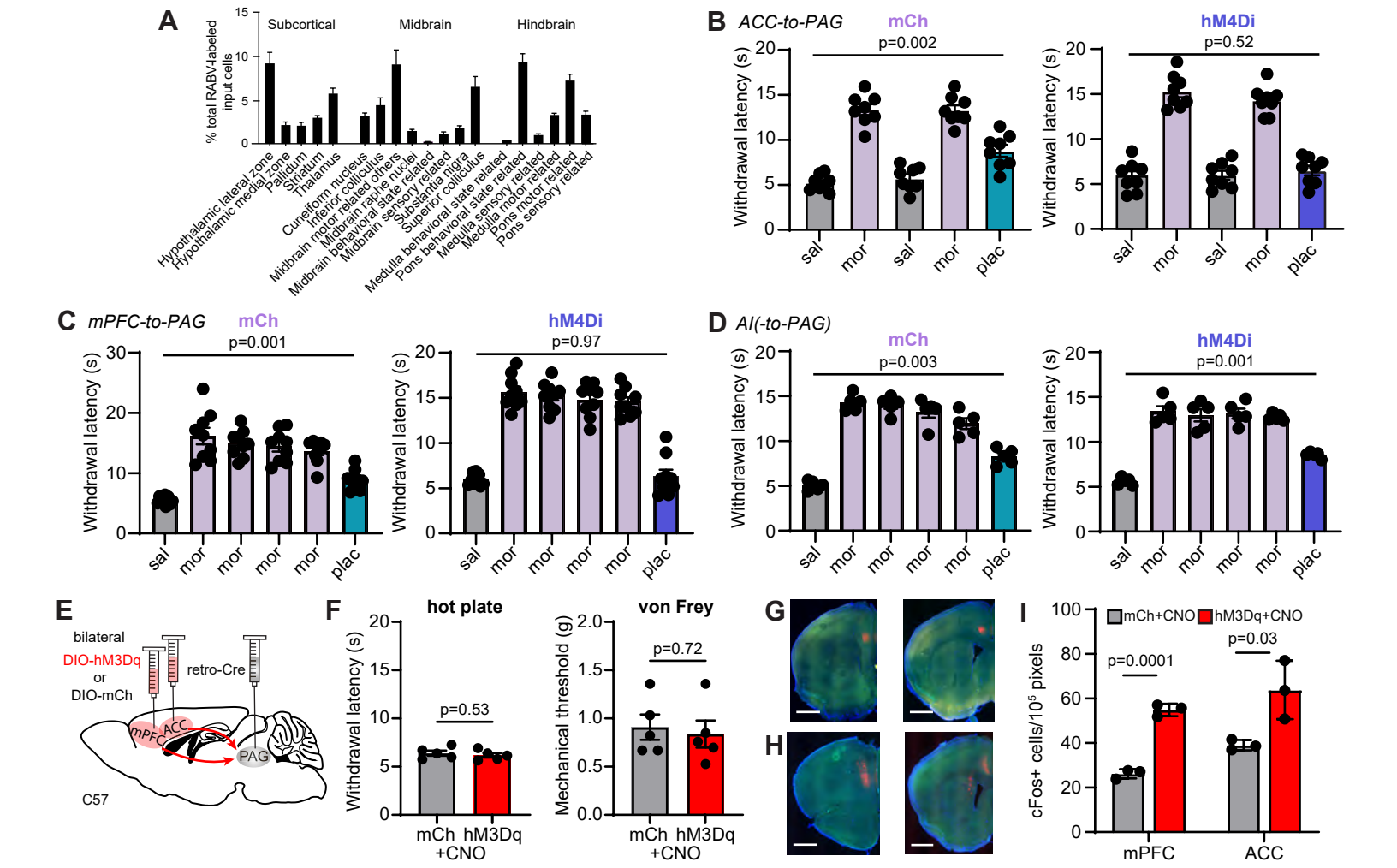
A
% total RABV-labeled input cells
Subcortical
Midbrain
Hindbrain
Hypothalamic lateral zone
Hypothalamic medial zone
Pallidum
Striatum
Thalamus
Cuneiform nucleus
Inferior colliculus
Midbrain motor related
Midbrain raphe nuclei
Midbrain behavioral state related
Midbrain sensory related
Substantia nigra
Superior colliculus
Medulla behavioral state related
Pons behavioral state related
Medulla sensory related
Medulla motor related
Pons motor related
Pons sensory related
B ACC-to-PAG
mCh
p=0.002
hM4Di
p=0.52
Withdrawal latency (s)
sal
mor
sal
mor
plac
C mPFC-to-PAG
mCh
p=0.001
hM4Di
p=0.97
D AI(-to-PAG)
mCh
p=0.003
hM4Di
p=0.001
E
bilateral
DIO-hM3Dq
or
DIO-mCh
retro-Cre
mPFC
ACC
PAG
C57
F
hot plate
p=0.53
Withdrawal latency (s)
von Frey
p=0.72
Mechanical threshold (g)
mCh +CNO
hM3Dq +CNO
G
H
I
mCh+CNO
hM3Dq+CNO
p=0.0001
p=0.03
cFos+ cells/10^5 pixels
mPFC
ACC

Figure S3. Chemogenetic inactivation of ACC→vlPAG, mPFC→vlPAG, and the vlPAG-projecting region of AI during the placebo test and simultaneous bilateral chemogenetic activation of mPFC→vlPAG and ACC→vlPAG neurons, Related to Figure 3. (**A**) Plot summarizing the subcortical regions identified as providing synaptic input to vlPAG→RVM neurons (n=6 mice). (**B**) Hot plate paw withdrawal latencies before, during, and after conditioning upon chemogenetic silencing of ACC→vlPAG neurons on placebo test day (mCh: n=8, RM one-way ANOVA with Dunnett's post-hoc, $F(2.25,15.73)=67.24$, $p<0.0001$; hM4Di: n=8, RM one-way ANOVA with Dunnett's post-hoc, $F(2.42,16.92)=93.54$, $p<0.0001$). (**C**) Hot plate paw withdrawal latencies before, during, and after conditioning upon chemogenetic silencing of mPFC→vlPAG neurons on placebo test day (mCh: n=9, RM one-way ANOVA with Dunnett's post-hoc, $F(2.08,16.63)=63.68$, $p<0.0001$; hM4Di: n=9, RM one-way ANOVA with Dunnett's post-hoc, $F(2.65,21.23)=113.8$, $p<0.0001$). (**D**) Hot plate paw withdrawal latencies before, during, and after conditioning upon chemogenetic silencing of the vlPAG-projecting region of AI on placebo test day (mCh: n=5, RM one-way ANOVA with Dunnett's post-hoc, $F(3.23,12.90)=126.9$, $p<0.0001$); hM4Di: n=5, RM one-way ANOVA with Dunnett's post-hoc, $F(2.09,8.37)=59.75$, $p<0.0001$). (**E**) Illustration of the retrograde viral injection approach for chemogenetic activation of mPFC→PAG and ACC→PAG neurons. (**F**) Paw withdrawal latencies on the hot plate (left) and mechanical thresholds to stimulation with von Frey fibers (right) upon chemogenetic activation of both ACC→PAG and mPFC→PAG neurons with hM3Dq vs. mCherry control (mCh: n=5, hM3Dq: n=5, unpaired t-tests). (**G**) Representative images of viral hM3Dq-mCh expression with cFos stained cells in the mPFC (left, scale bar = 750 μm) and ACC (right, scale bar = 750 μm). (**H**) Same as in (**G**), but for mCh. (**I**) Graph showing number of cFos-

positive cells within the mPFC and ACC, quantified by number of cFos-positive cells within $1x10^5$ pixel bins. ROIs were limited to the mPFC or ACC (mCh control: n=3, hM3Dq-mCh: n=3, unpaired t-test).

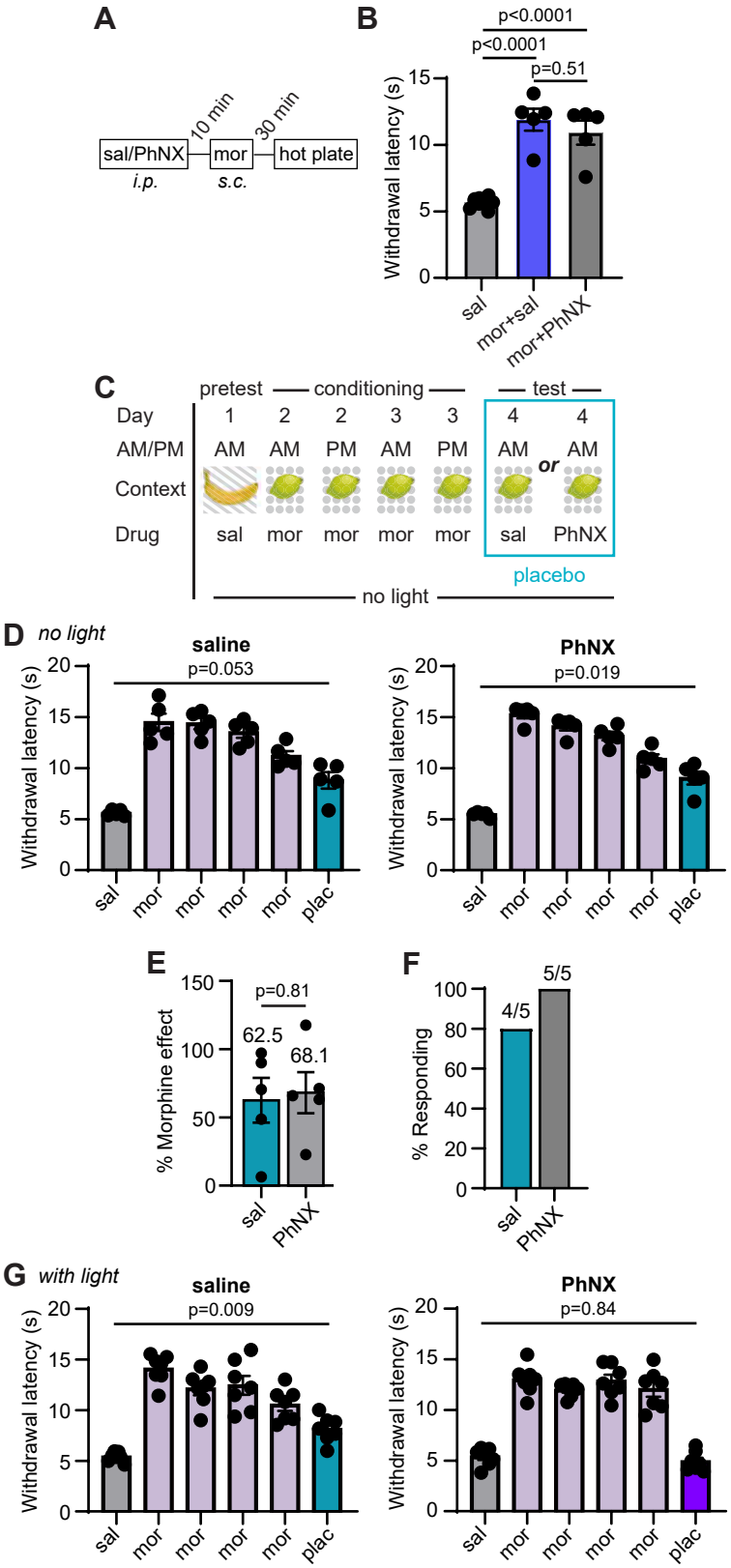
A
sal/PhNX
i.p.
10 min
mor
s.c.
30 min
hot plate
B
p<0.0001
p<0.0001
p=0.51
Withdrawal latency (s)
sal
mor+sal
mor+PhNX
C
pretest
conditioning
test
Day
AM/PM
Context
Drug
sal
mor
or
PhNX
placebo
no light
D no light
saline
p=0.053
PhNX
p=0.019
Withdrawal latency (s)
plac
E
p=0.81
62.5
68.1
% Morphine effect
F
4/5
5/5
% Responding
G with light
saline
p=0.009
PhNX
p=0.84

Figure S4: PhNX is inactive in the absence of light, Related to Figure 4.

(**A**) Schematic of PhNX (30 mg/kg *i.p.*) and morphine (5 mg/kg *s.c.*) administration to assess potential antagonism of opioid signaling by PhNX *in vivo*. (**B**) Paw withdrawal latencies on the hot plate in response to saline, morphine and saline, or morphine and PhNX (saline: n=10, mor+sal: n=5, mor+PhNX: n=5, One-way ANOVA with Tukey's post-hoc, $F(2,17)=44.81$, $p<0.0001$). (**C**) Schematic of Protocol 2 with administration of either saline or PhNX (30 mg/kg *i.p.*) on test day in the absence of photoactivation. (**D**) Hot plate paw withdrawal latencies before, during, and after conditioning in the absence and presence of PhNX without light (sal: n=5, RM one-way ANOVA with Dunnett's post-hoc, $F(1.83,7.30)=30.18$, $p=0.0003$; PhNX: n=5, RM one-way ANOVA with Dunnett's post-hoc, $F(2.16,8.64)=76.96$, $p<0.0001$). (**E**) Placebo effect quantified as % of the response to the previous dose of morphine (saline: n=5, PhNX: n=5, unpaired t-test). (**F**) Placebo response quantified as the % of subjects exhibiting antinociception. (**G**) Hot plate paw withdrawal latencies before, during, and after conditioning in the absence and presence of PhNX and light (sal: n=7, RM one-way ANOVA with Dunnett's post-hoc, $F(2.39,14.34)=26.91$, $p<0.0001$); PhNX: n=7, RM one-way ANOVA with Dunnett's post-hoc, $F(2.91,17.47)=69.55$, $p<0.0001$).

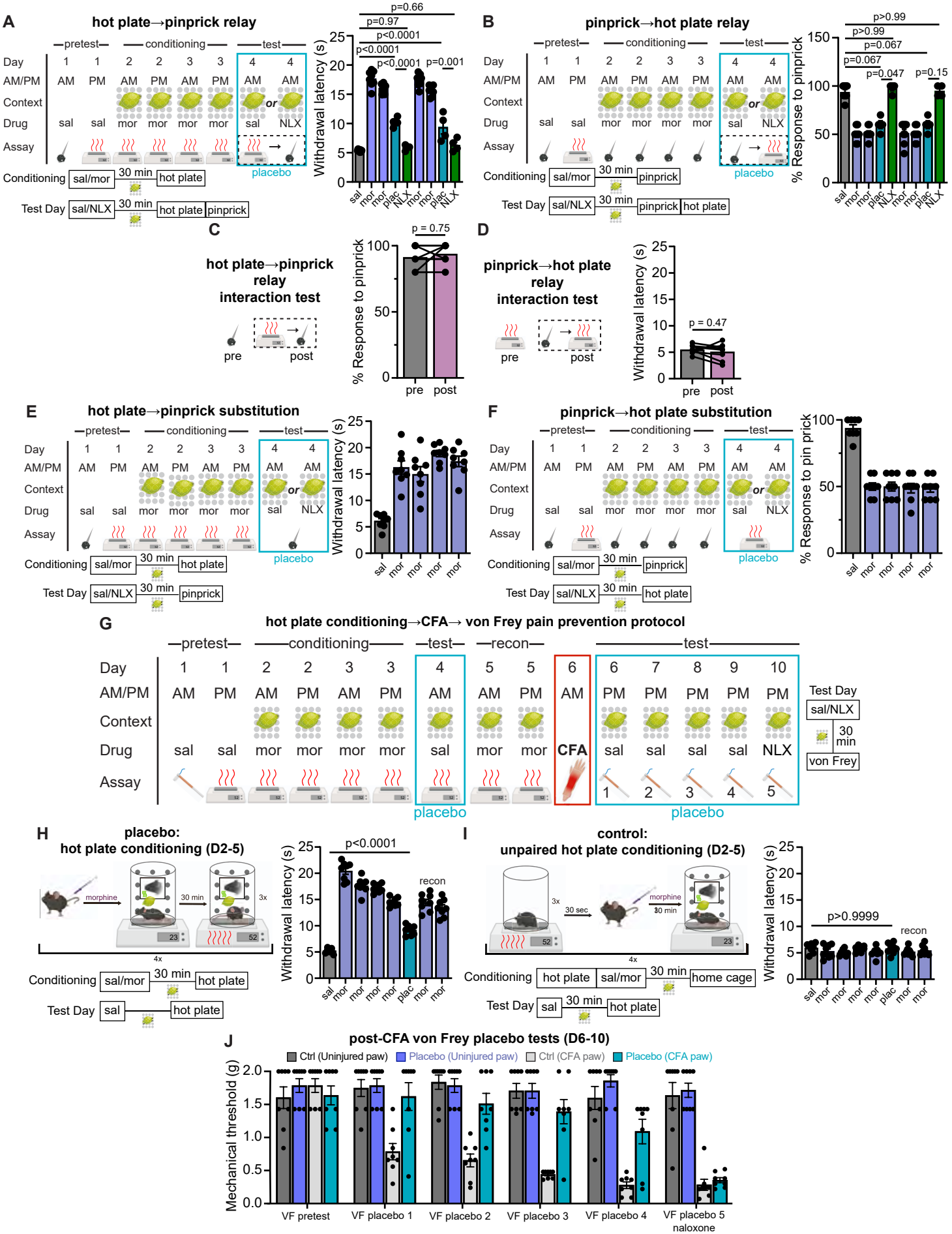
A
hot plate→pinprick relay
pretest
conditioning
test
Day
AM/PM
Context
Drug
Assay
sal
mor
or
NLX
placebo
Conditioning
sal/mor
30 min
hot plate
Test Day
sal/NLX
pinprick
Withdrawal latency (s)
p=0.66
p=0.97
p<0.0001
p<0.0001
p<0.0001
p=0.001
B
pinprick→hot plate relay
% Response to pinprick
p>0.99
p>0.99
p=0.067
p=0.067
p=0.047
p=0.15
C
hot plate→pinprick relay interaction test
pre
post
p = 0.75
D
pinprick→hot plate relay interaction test
p = 0.47
E
hot plate→pinprick substitution
F
pinprick→hot plate substitution
% Response to pin prick
G
hot plate conditioning→CFA→ von Frey pain prevention protocol
recon
CFA
Test Day
von Frey
H
placebo:
hot plate conditioning (D2-5)
morphine
3x
4x
I
control:
unpaired hot plate conditioning (D2-5)
30 sec
home cage
J
post-CFA von Frey placebo tests (D6-10)
Ctrl (Uninjured paw)
Placebo (Uninjured paw)
Ctrl (CFA paw)
Placebo (CFA paw)
Mechanical threshold (g)
VF pretest
VF placebo 1
VF placebo 2
VF placebo 3
VF placebo 4
VF placebo 5
naloxone

Figure S5: Pain modality transfer conditioning data, Related to Figure 5.

(**A**) (left) Schematic of the hot plate→pinprick relay conditioning protocol. (right) Hot plate withdrawal latencies before, during, and after conditioning for the hot plate→pinprick relay experiment (n=8, one-way ANOVA with Sidak's post-hoc $F(8,47)=149.5$, $p<0.0001$). (**B**) (left) Schematic of the pinprick→ hot plate relay conditioning protocol. (right) Responses measured as number of responses to 10 pinpricks before, during, and after conditioning for the pinprick→hot plate relay experiment (n=8, Kruskal-Wallis test, $H=16.88$, $p=0.0020$ with Dunn's post-hoc). (**C**) (left) Schematic of the hot plate→pinprick relay interaction test. (right) Pinprick responses before (pre) and immediately after (post) the hot plate test (n=8, Wilcoxon matched-pairs signed rank test). (**D**) (left) Schematic of the pinprick→ hot plate relay interaction test. (right) Hot plate latencies before (pre) and immediately after (post) the pinprick test (n=8 mice, paired t-test). (**E**) (left) Schematic of the hot plate→pinprick substitution conditioning protocol. (right) Hot plate withdrawal latencies before and during conditioning for the hot plate→pinprick substitution experiment (n=8). (**F**) (left) Schematic of the pinprick→ hot plate substitution conditioning protocol. (right) Pinprick responses before and during conditioning for the pinprick→hot plate substitution experiment (n=8). (**G**) Schematic of the hot plate→CFA→von Frey pain-prevention conditioning protocol. (**H**) (left) Schematic of the placebo conditioning sequence that pairs morphine with context and noxious stimulus presentation on the hot plate. (right) Hot plate withdrawal latencies before, during, and after conditioning for the hot plate-paired placebo group in the pain prevention experiment (n=8 mice total, RM one-way ANOVA with Tukey's post-hoc, $F(7,56)=112.2$, $p<0.0001$). (**I**) (left) Schematic of the

control unpaired conditioning sequence that pairs morphine with context but not the hot plate. (right) Hot plate withdrawal latencies before, during, and after conditioning for the unpaired control group in the pain prevention experiment (n=8 mice total, RM one-way ANOVA with Tukey's post-hoc, $F(7,56)=1.228$, $p=0.30$). (**J**) Von Frey mechanical thresholds for individual mice in the pain prevention experiment (n=16 mice total, unpaired: n=8, paired: n=8).